



CTU

CZECH TECHNICAL
UNIVERSITY
IN PRAGUE

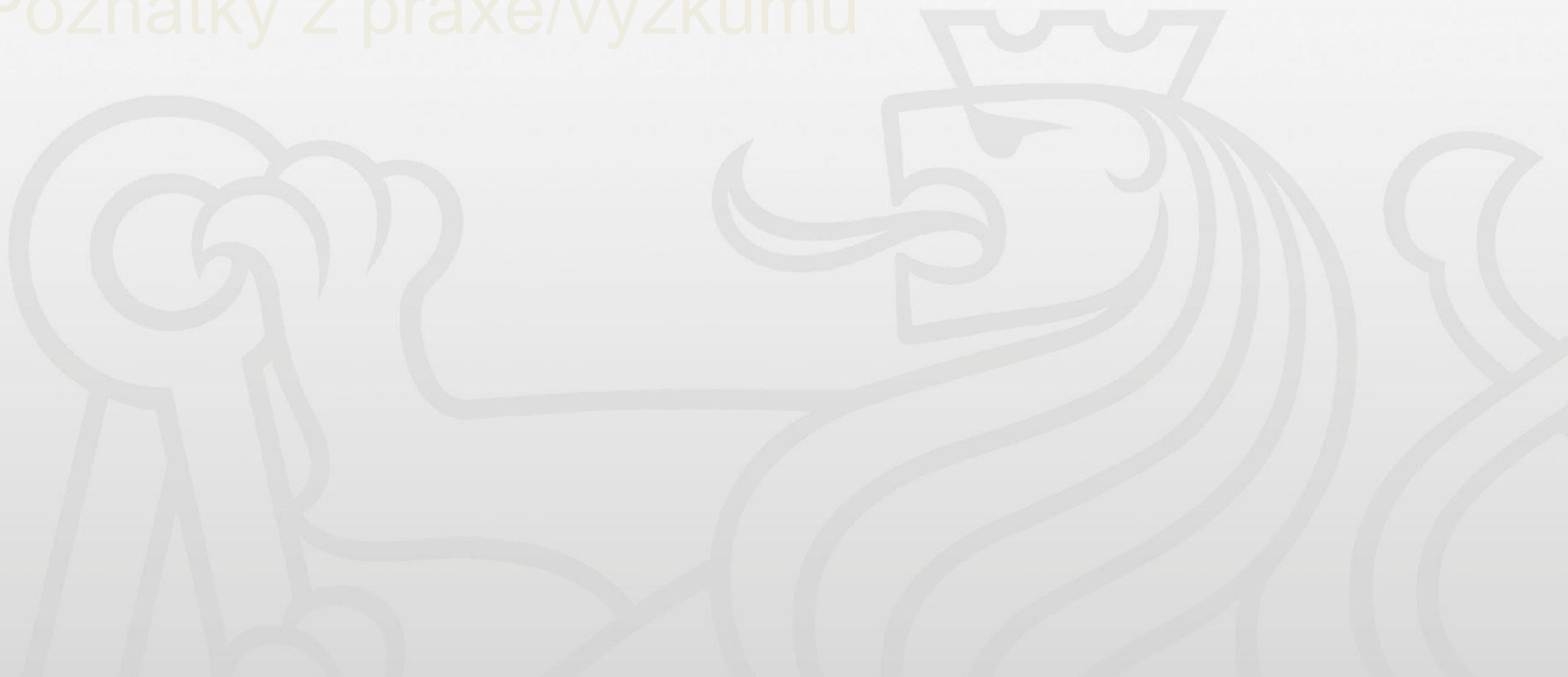
Výkon nebo bezpečnost Efektivní kolaborativní robotika

Petr Švarný
Katedra kybernetiky
FEL ČVUT

Seminář Robotika.sk 2022

1. Co je to Cobot?
2. Teorie bezpečné kolaborace, alias 15066
3. Poznatky z praxe a výzkumu

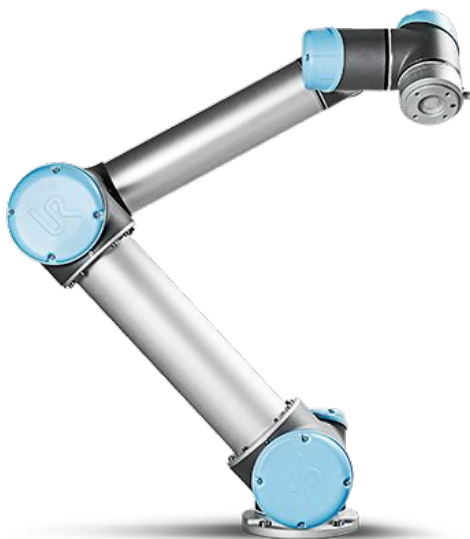
1. Co je to Cobot?
2. Teorie bezpečné kolaborace, alias 15066
3. Poznatky z praxe/výzkumu



Collaborative robot alias Cobot

Robot	Cobot
Malá variabilita, velké dávky	Malé dávky, vysoká variabilita
Složité nasazení	Lehké nasazení
Není bezpečný	Kolaborativní a bezpečný
Integrovaný robot i s nástrojem pro úlohu	Hlavní je nástroj
Velká investice, pomalá návratnost	Menší investice, rychlejší návratnost

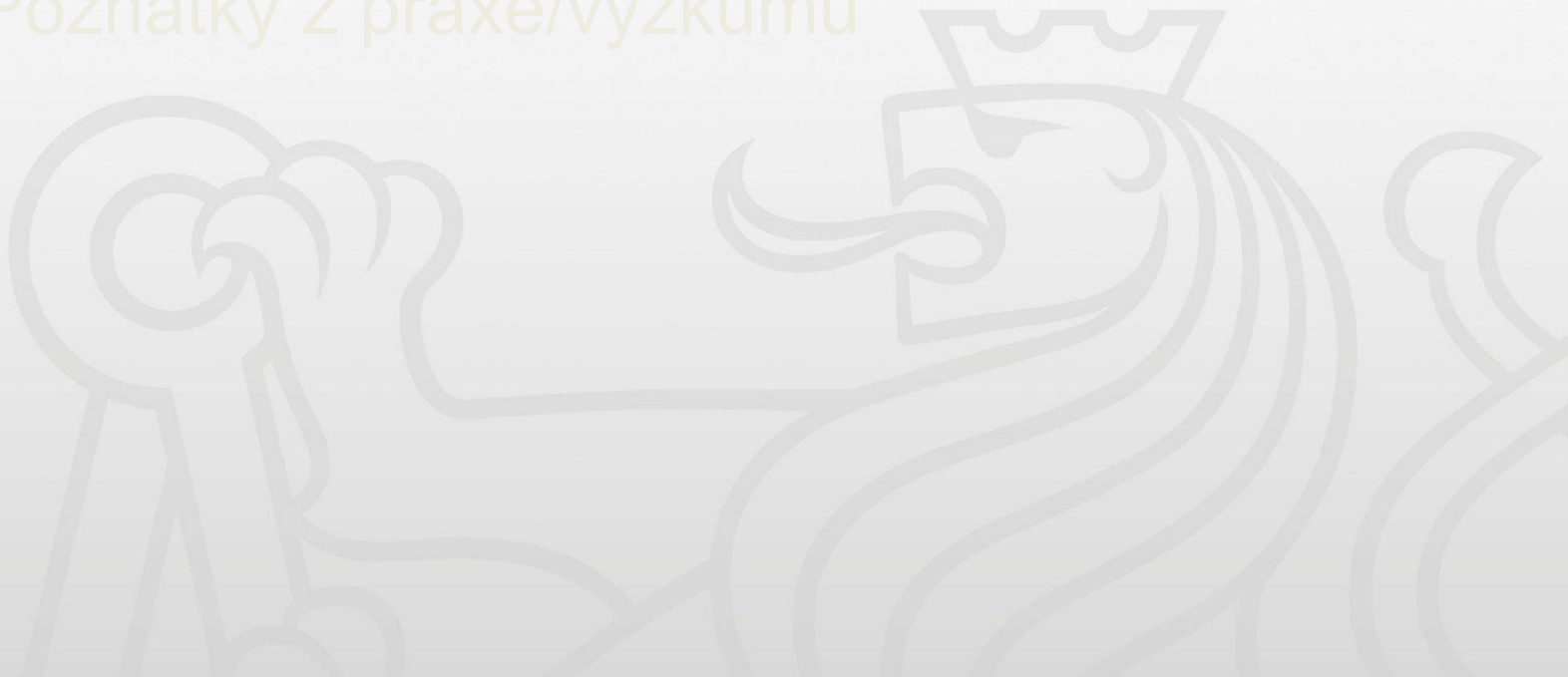
Nejznámnější koboti



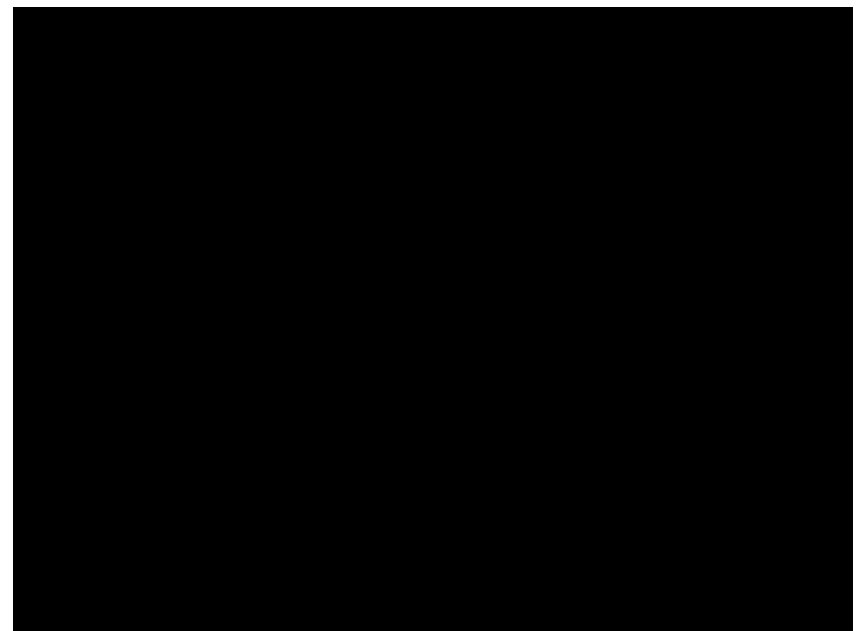
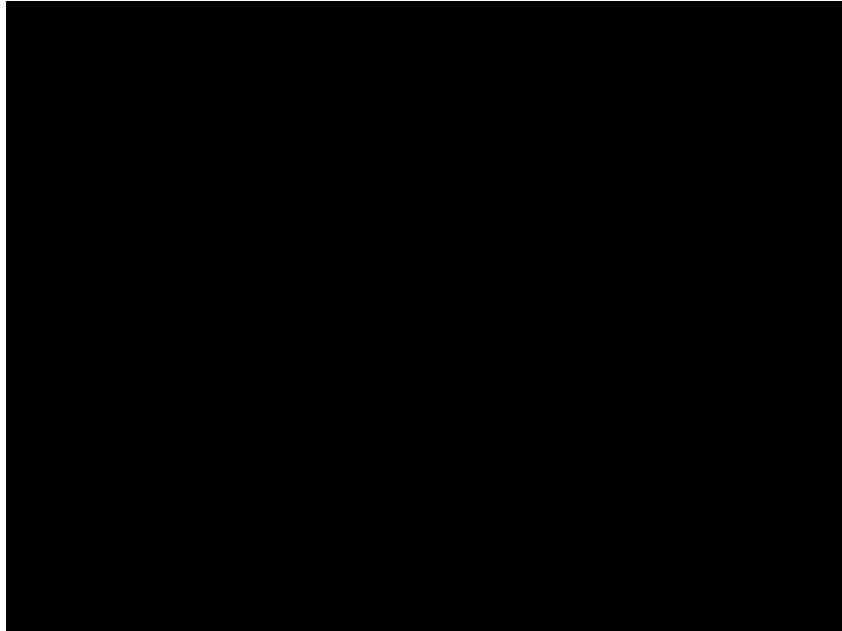
Collaborative robot alias Cobot

Robot	Cobot
Malá variabilita, velké dávky	Malé dávky, vysoká variabilita
Složité nasazení	Lehké nasazení
Není bezpečný	Kolaborativní a bezpečný
Integrovaný robot i s nástrojem pro úlohu	Hlavní je nástroj
Velká investice, pomalá návratnost	Menší investice, rychlejší návratnost

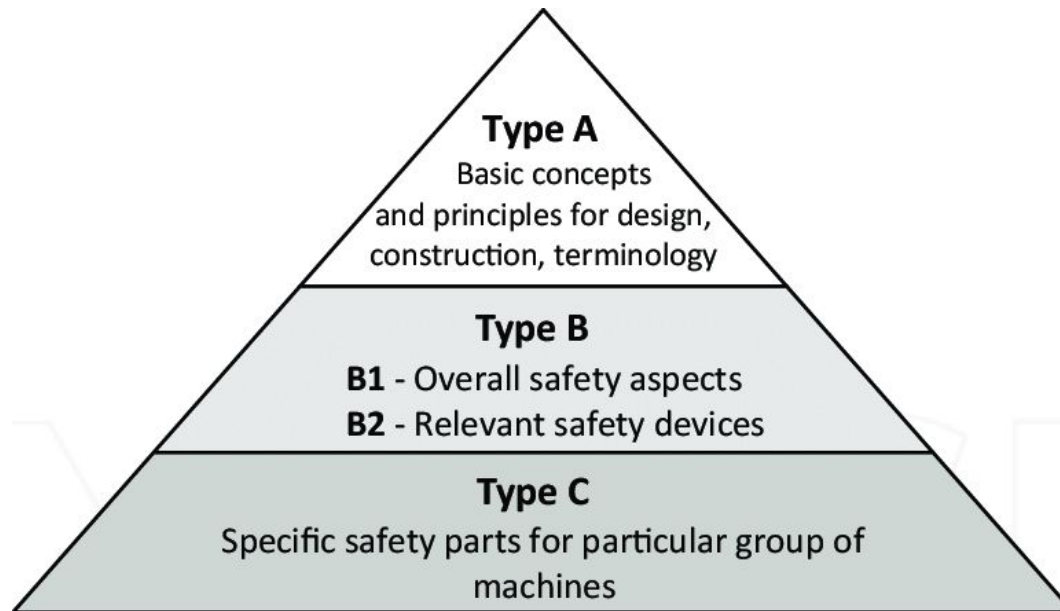
1. Co je to Cobot?
2. Teorie bezpečné kolaborace, alias 15066
3. Poznatky z praxe/výzkumu



Bezpečnost robota



Bezpečnostní standardy



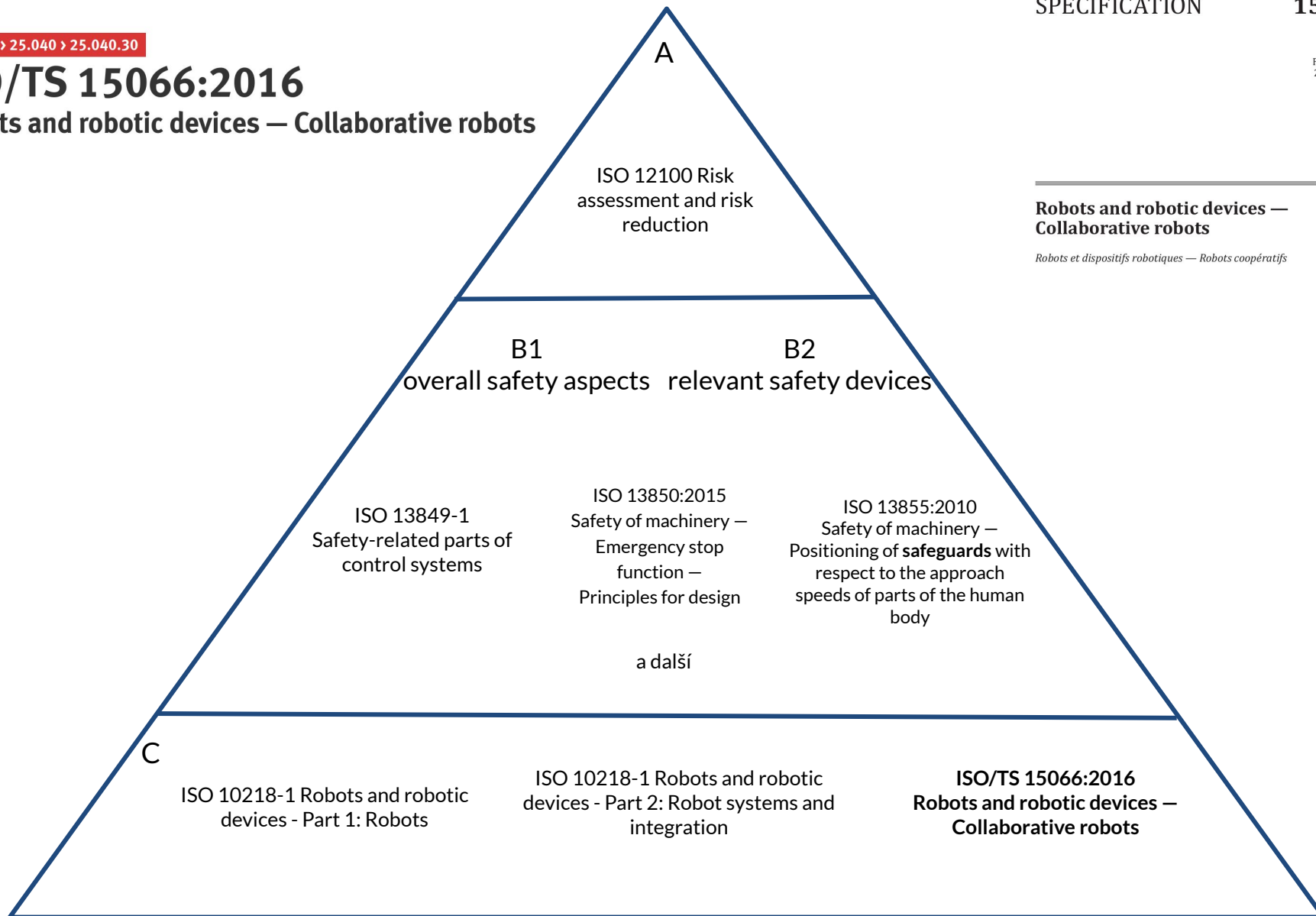
Pacaiova, H. (2018). *Machinery safety requirements as an effective tools for operational safety management*. IntechOpen.

Převzato a upraveno ze slidů M. Hoffmanna - kurz Humanoidní roboti, ČVUT FEL

ICS > 25 > 25.040 > 25.040.30

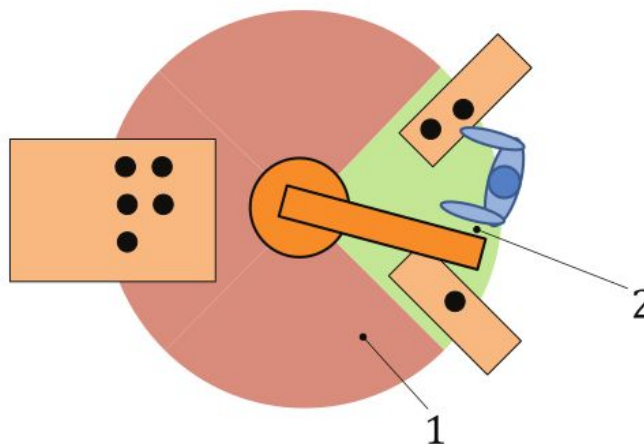
ISO/TS 15066:2016

Robots and robotic devices — Collaborative robots



Robots and robotic devices — Collaborative robots

Robots et dispositifs robotiques — Robots coopératifs



Key

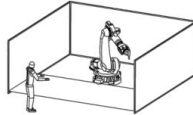
- 1 operating space
- 2 collaborative workspace

Figure 1 — Example of a collaborative workspace

ISO 10218-2 – Types of human-robot-collaboration

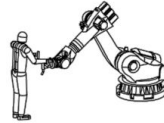
1. Safety-rated monitored stop

- Robot in normal automatic mode
- Robot stops when human enters the workspace and resumes automatically after leaving



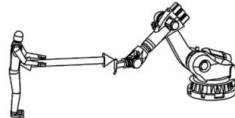
2. Hand guided operation

- Robot operates at low speed
- Operation only with enabling switch



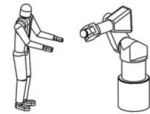
3. Speed and separation monitoring

- Robot operates autonomously at low speed
- Robot stops when distance to human gets too small



4. Power and force limiting

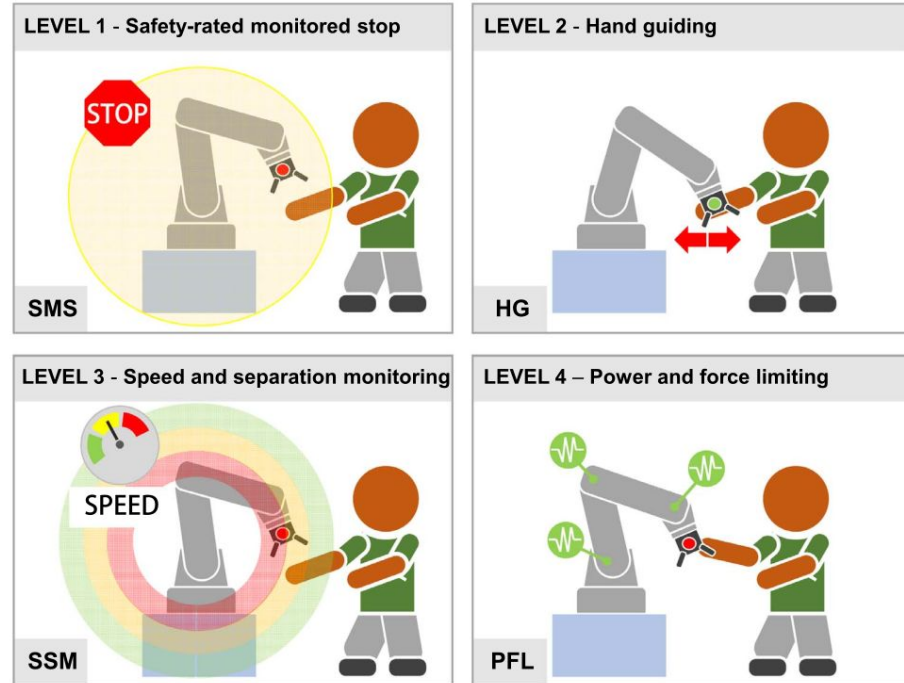
- Restriction of force and power of the robot
- Contact between human and robot allowed



14

© Fraunhofer IPA 2015

Theo Jacobs, Fraunhofer IPA, Safety standards and risk assessment for robots, 2016



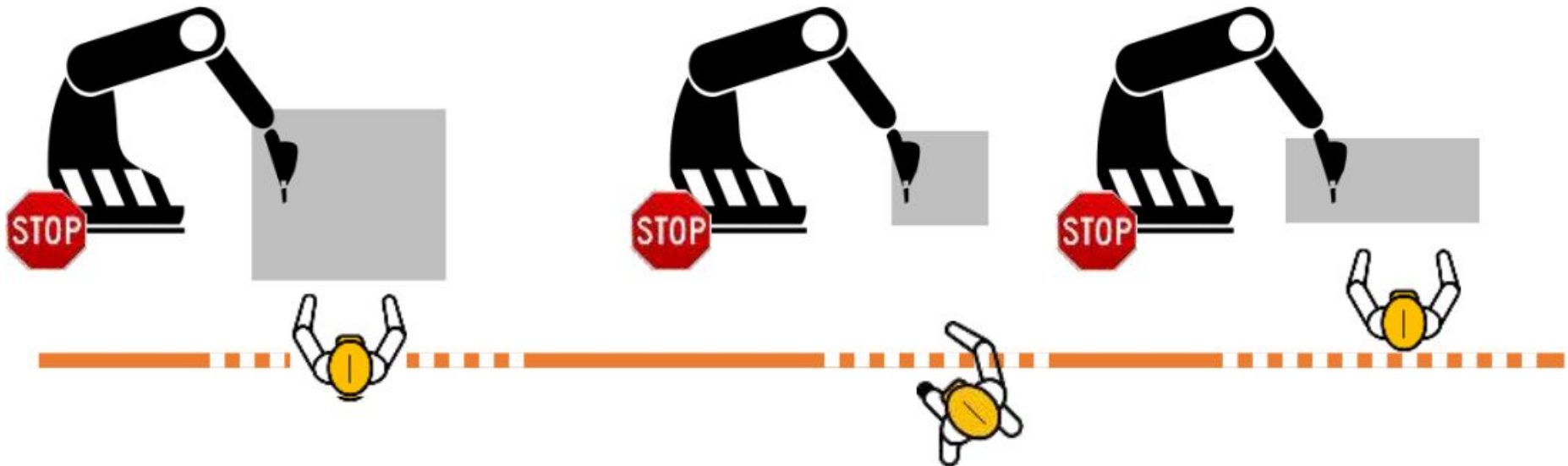
Villani, V., Pini, F., Leali, F., & Secchi, C. (2018). Survey on human–robot collaboration in industrial settings: Safety, intuitive interfaces and applications. *Mechatronics*, 55, 248-266.

Design 0 - tradiční



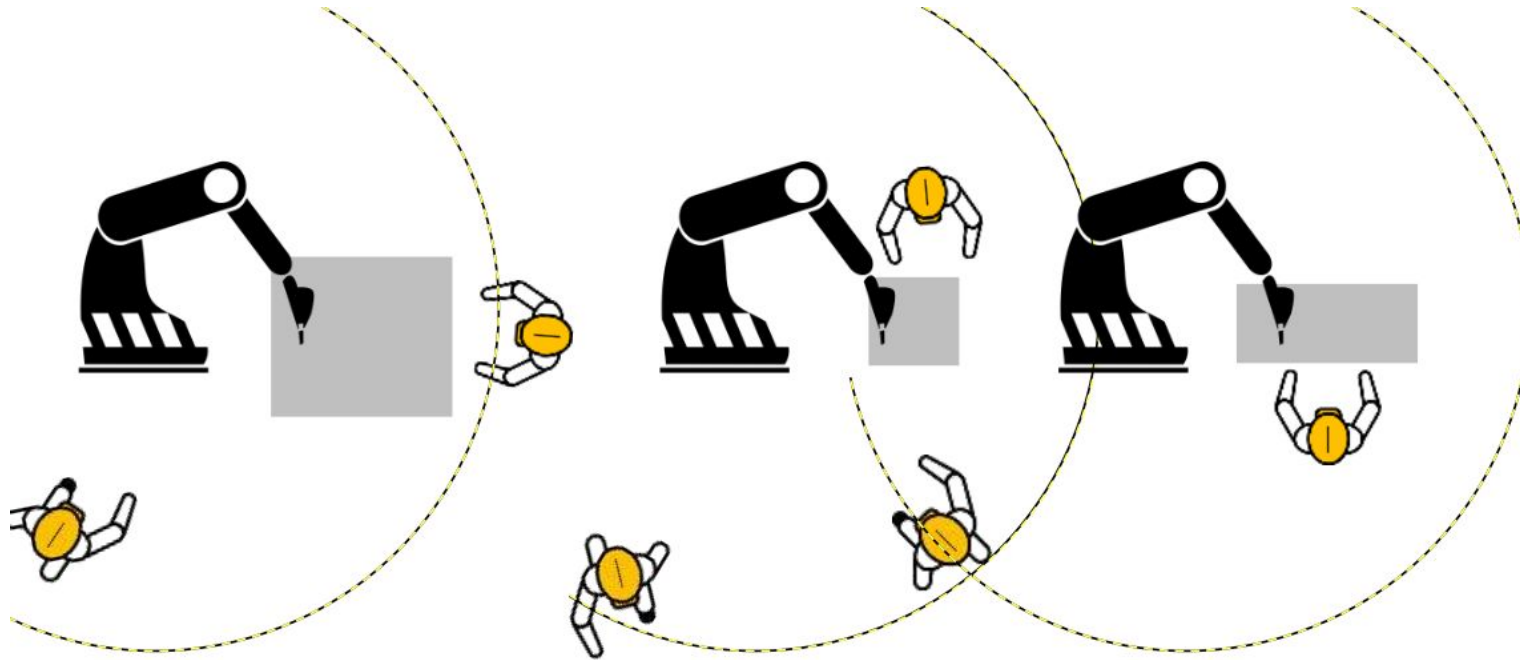
Slide from F. Vicentini: Safety of collaborative robotics. Speed and separation monitoring @ IROS 2018.

Design 1a - safety-rated monitored stop



Slide from F. Vicentini: Safety of collaborative robotics. Speed and separation monitoring @ IROS 2018.

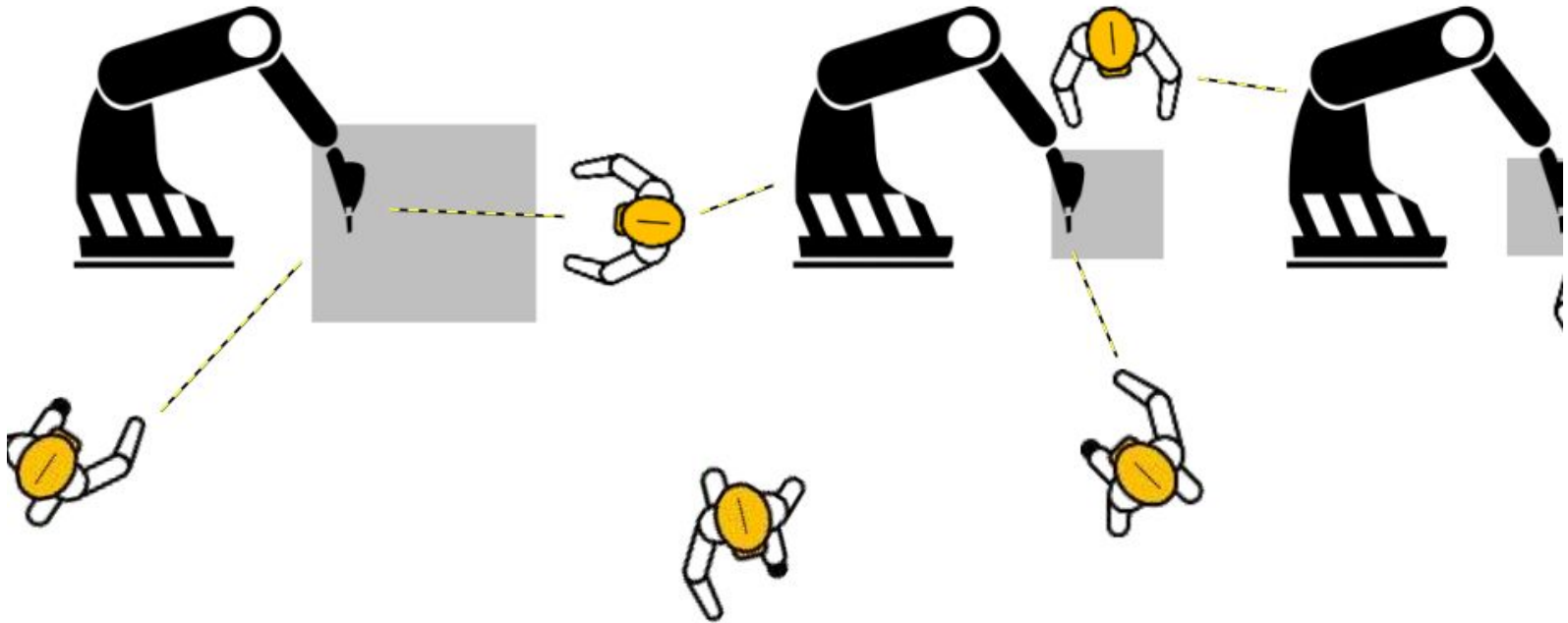
Design 1b - safety-rated monitored stop



large footprint
low flexibility

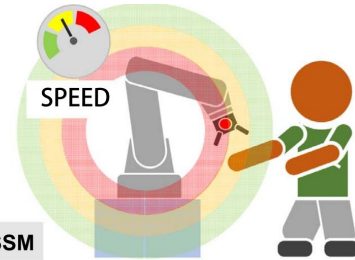
Slide from F. Vicentini: Safety of collaborative robotics. Speed and separation monitoring @ IROS 2018.

Design 3 - SSM



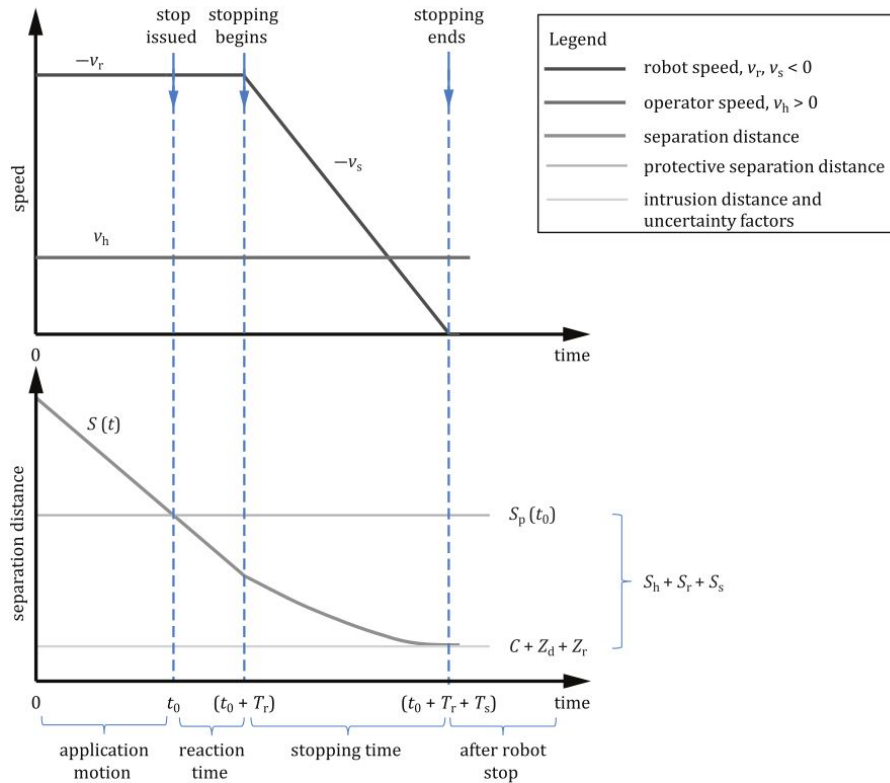
Slide from F. Vicentini: Safety of collaborative robotics. Speed and separation monitoring @ IROS 2018.

Speed and separation monitoring



ISO/TS 15066

Villani et al.
(2018)



The protective separation distance, S_p , can be described by Formula (1):

$$S_p(t_0) = S_h + S_r + S_s + C + Z_d + Z_r \quad (1)$$

where

$S_p(t_0)$ is the protective separation distance at time t_0 ;

t_0 is the present or current time;

S_h is the contribution to the protective separation distance attributable to the operator's change in location;

S_r is the contribution to the protective separation distance attributable to the robot system's reaction time;

S_s is the contribution to the protective separation distance due to the robot system's stopping distance;

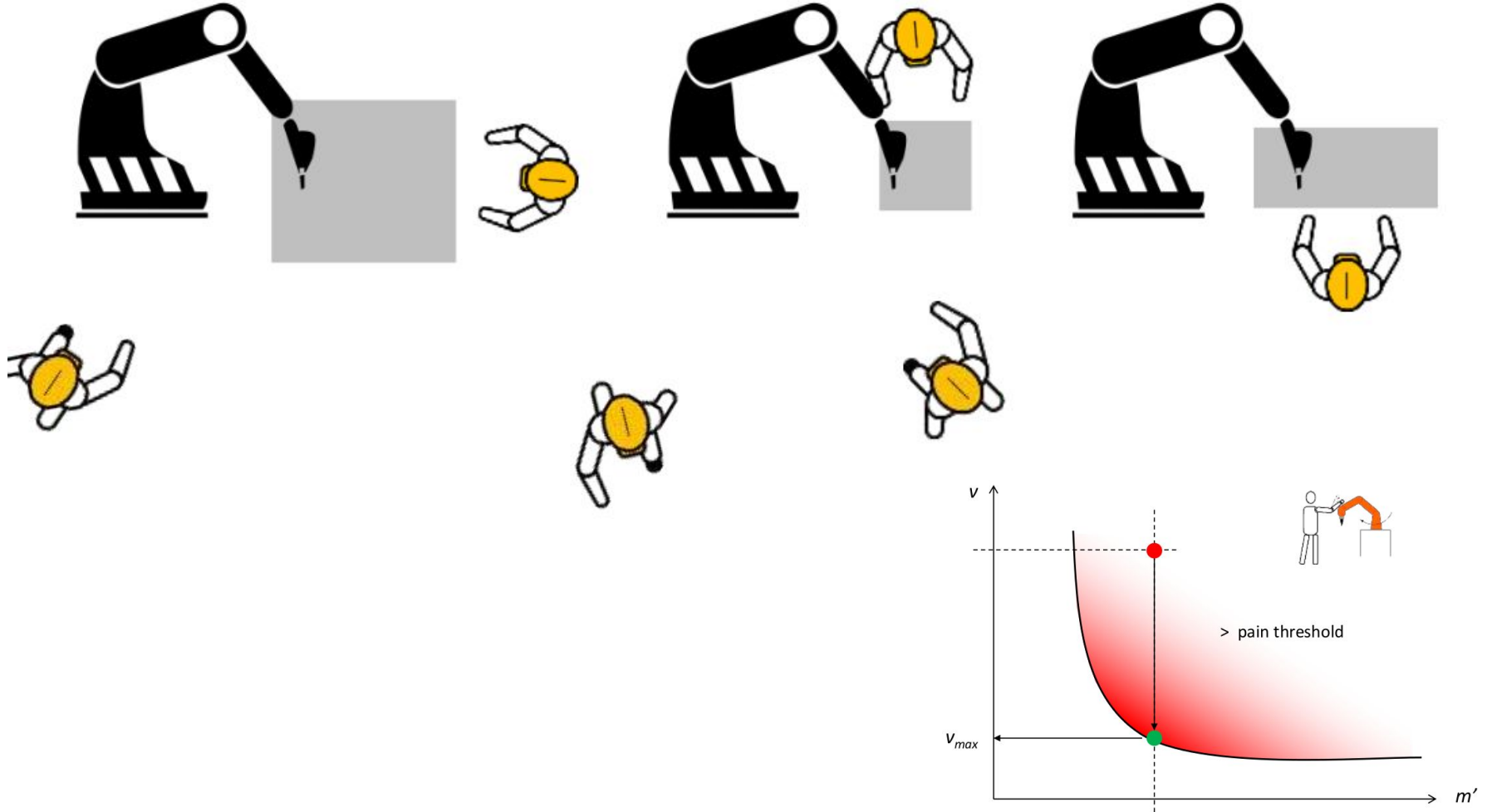
C is the intrusion distance, as defined in ISO 13855; this is the distance that a part of the body can intrude into the sensing field before it is detected;

Z_d is the position uncertainty of the operator in the collaborative workspace, as measured by the presence sensing device resulting from the sensing system measurement tolerance;

Z_r is the position uncertainty of the robot system, resulting from the accuracy of the robot position measurement system.

Figure 3 — Graphical representation of the contributions to the protective separation distance between an operator and a robot

Design 4 - PFL



Slide from F. Vicentini: Safety of collaborative robotics. Speed and separation monitoring @ IROS 2018.

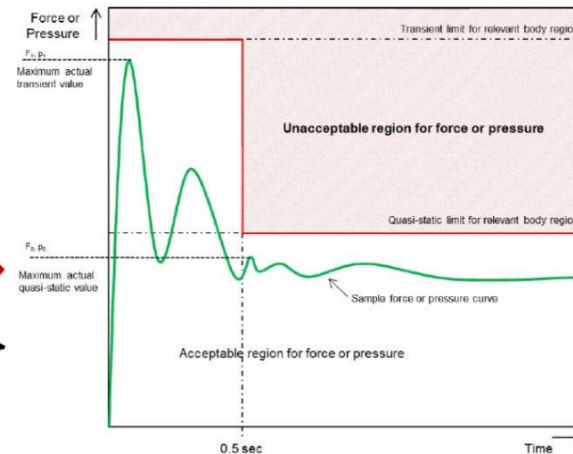
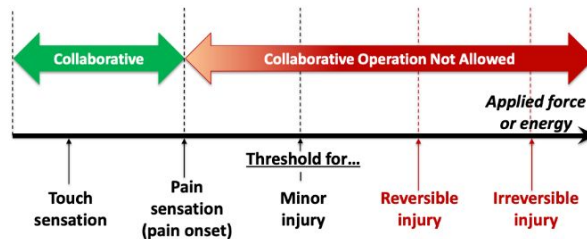
Biomechanical criteria in TS 15066



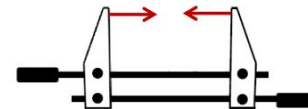
80 W/150 N power and force limits were present in ISO 10218-1:2006 but have been removed in 2011!

$$1 W = 1 N \frac{m}{s} = 1 \frac{kg m^2}{s^3}$$

↓
"onset of pain" studies
↓



- force applied where (body part)?
- clamping conditions?

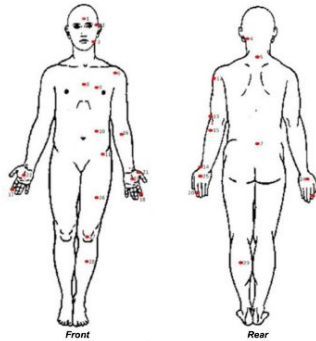


pHRI

51

Slide from Alessandro de Luca: Physical HRI. http://www.diag.uniroma1.it/deluca/pHRI_elective/pHRI_SafetyDependability.pdf

Biomechanical criteria in TS 15066



Body Region	Specific Body Area	Quasi-Static Contact		Transient Contact	
		Maximum Allowable Pressure p_a [N/cm ²] (see NOTE 1)	Maximum Allowable Force [N] (see NOTE 2)	Maximum Allowable Pressure Multiplier F_T (see NOTE 3)	Maximum Allowable Force Multiplier F_r (see NOTE 3)
Skull and forehead	1 Middle of forehead	125	125	N/A	N/A
	2 Temple	115	130	N/A	N/A
Face	3 Masticatory muscle	110	65	N/A	N/A
Neck	4 Neck muscle	138	145	2	2
	5 Seventh neck muscle	205		2	
Back and shoulders	6 Shoulder joint	155	210	2	2
	7 Fifth lumbar vertebra	213		2	2
Chest	8 Sternum	116	140	2	2
	9 Pectoral muscle	166		2	2
Abdomen	10 Abdominal muscle	143	110	2	2
Pelvis	11 Pelvic bone	209	180	2	2
Upper arms and elbow joints	12 Deltoid muscle	192	150	2	2
	13 Humerus	216		2	
Lower arms and wrist joints	14 Radial bone	192		2	
	15 Forearm muscle	181	160	2	2
	16 Arm nerve	179		2	
Hands and fingers	17 Forefinger pad D	298		2	
	18 Forefinger pad ND	273		2	
	19 Forefinger end joint D	275		2	
	20 Forefinger end joint ND	219		2	
	21 Thenar eminence	203	135	2	2
	22 Palm D	256		2	
	23 Palm ND	260		2	
	24 Back of the hand D	197		2	
	25 Back of the hand ND	193		2	
Thighs and knees	26 Thigh muscle	246	220	2	2
	27 Kneecap	223		2	
Lower legs	28 Middle of shin	220	125	2	2
	29 Calf muscle	212		2	

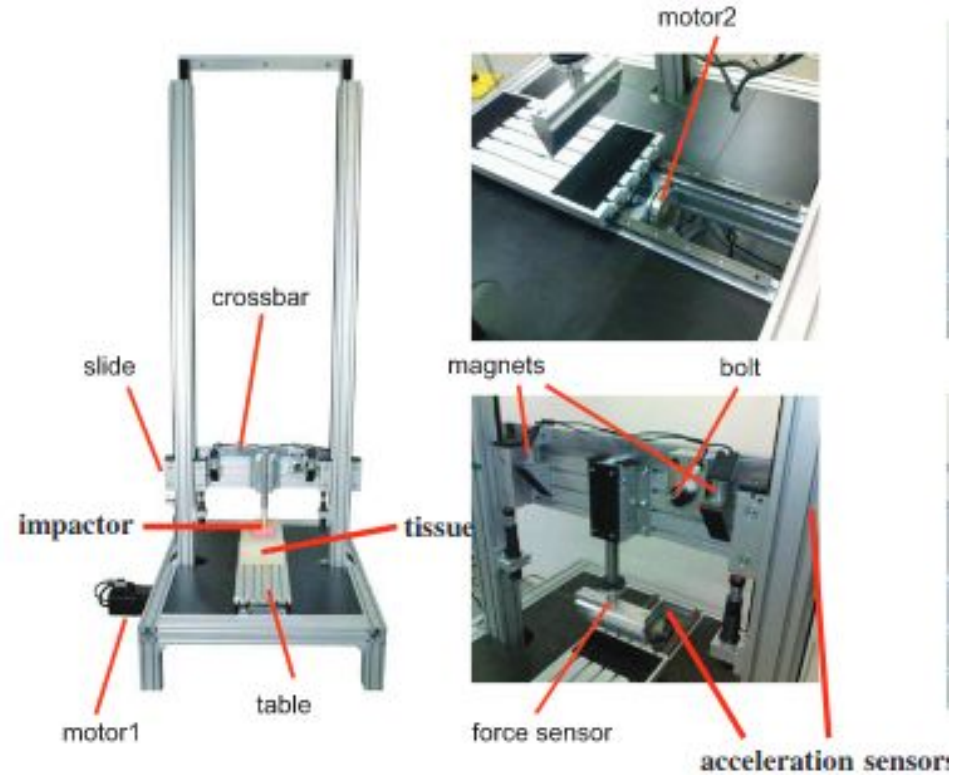
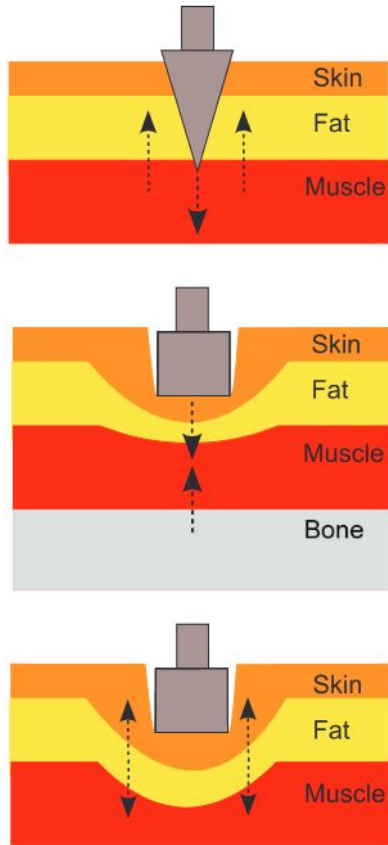
from studies by the University of Mainz

pHRI

52

Slide from Alessandro de Luca: Physical HRI. http://www.diag.uniroma1.it/deluca/pHRI_elective/pHRI_SafetyDependability.pdf

Vyhodnocení impaktoru

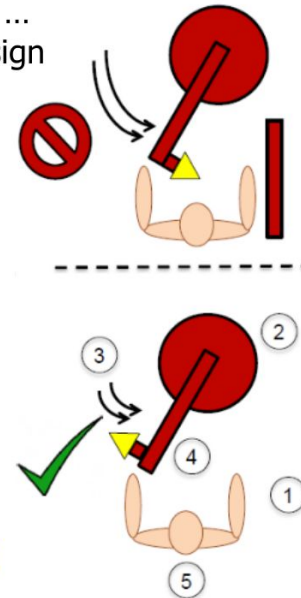


Modification of power and force limits



an example of risk critical task ...
mitigated by application re-design

1. Eliminate **pinch** and **crush** points
2. Reduce robot system **inertia** or **mass**
3. Reduce robot system **velocity**
2. & 3. will reduce energy transfer in a collision
4. Modify robot posture such that **contact surface area** is increased
5. Avoid sensitive body areas (head & neck)
- + Safe control: **collision detection & reaction**



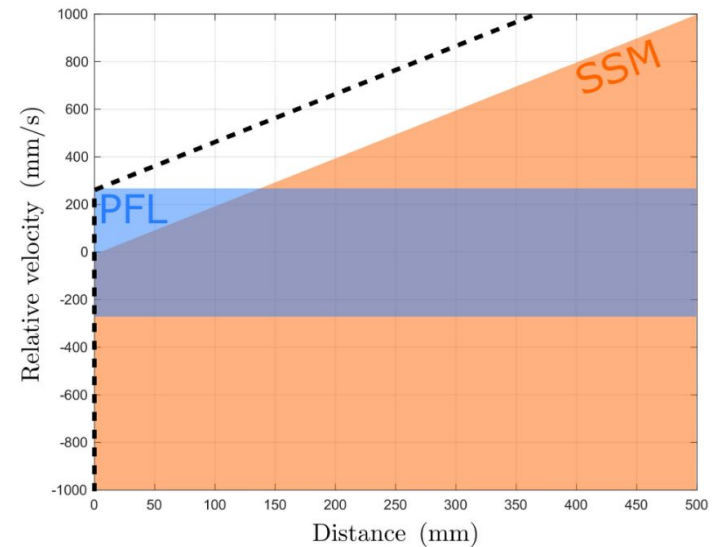
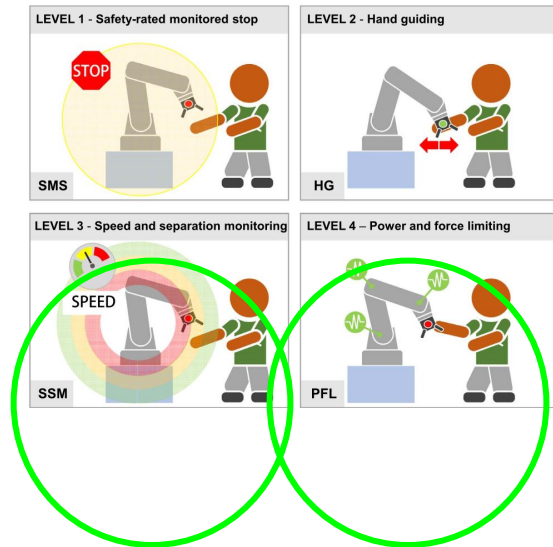
pHRI

58

Slide from Alessandro de Luca: Physical HRI. http://www.diag.uniroma1.it/deluca/pHRI_elective/pHRI_SafetyDependability.pdf

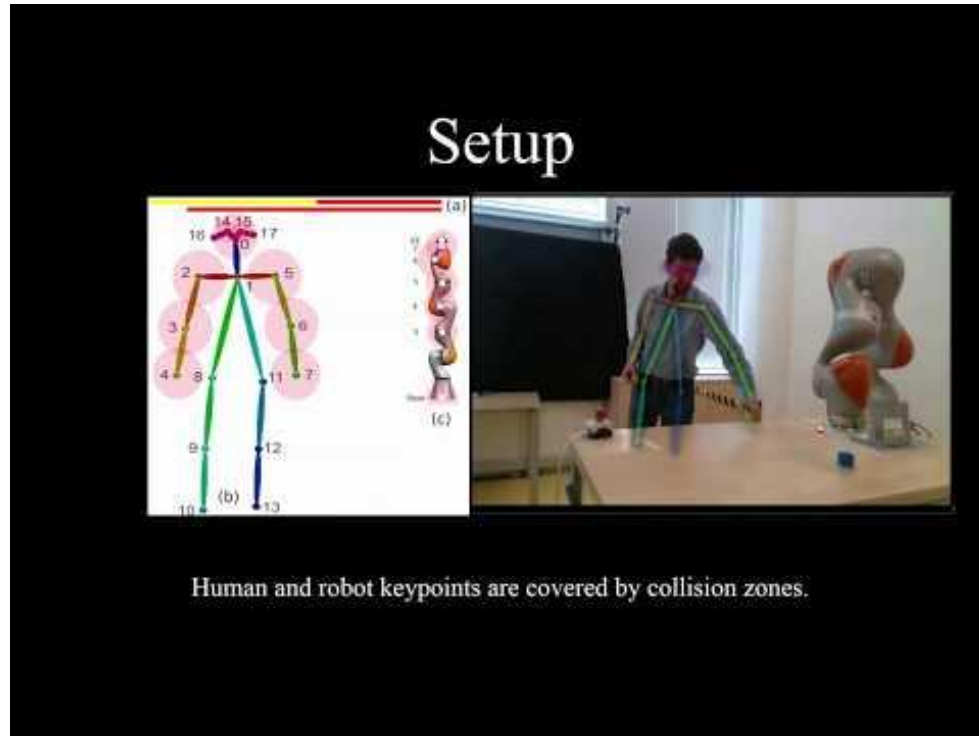
1. Co je to Cobot?
2. Teorie bezpečné kolaborace, alias 15066
3. Poznatky z praxe a výzkumu
 - a. PFL a SSM
 - b. 3D CFM - kolize dle konfigurace robotu
 - c. Airskin a kolize

Případová studie - Kombinace power and force limiting (PFL) a speed and separation monitoring (SSM)



Lucci, N., Lacevic, B., Zanchettin, A. M., & Rocco, P. (2020). Combining speed and separation monitoring with power and force limiting for safe collaborative robotics applications. *IEEE Robotics and Automation Letters*, 5(4), 6121-6128.

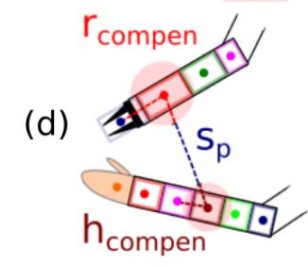
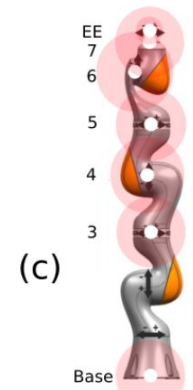
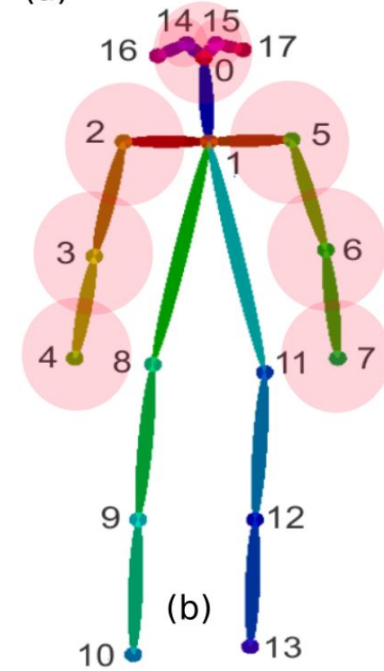
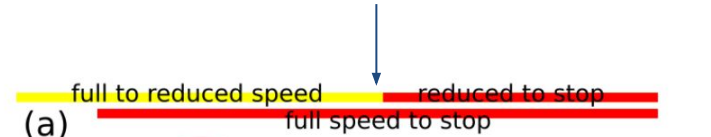
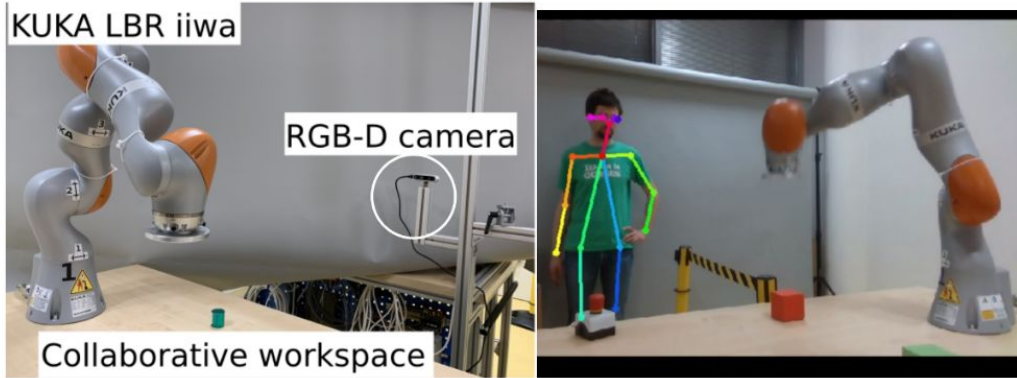
PFL & SSM



PFL & SSM

End-effector	Stop	from	Reduce	speed	Stop	from
	full	speed	Nose	Wrist	reduced	speed
Nose	1.28	1.33	1.44	1.49	0.71	0.76
3	1.33	1.38	1.49	1.54	0.76	0.81
Base	1.28	1.33	1.44	1.49	0.71	0.76

TABLE II: Effective keypoint-pair protective separation distance in meters.

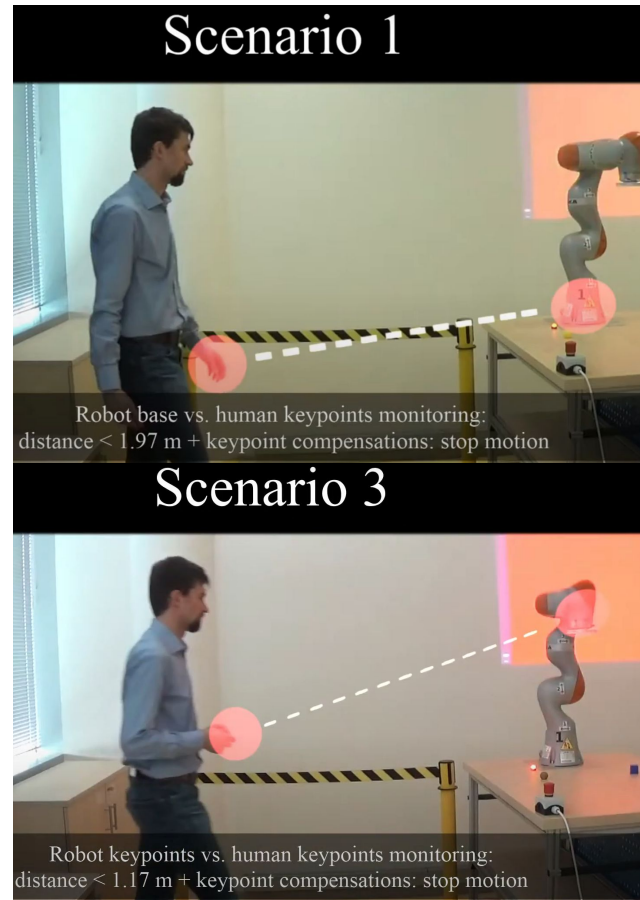
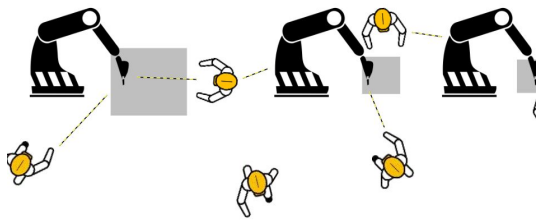
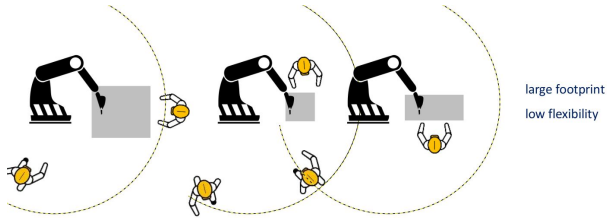


Separation distance z ISO/TS 15066:

$$S_p(t_0) = S_h + S_r + S_s + C + Z_d + Z_r$$

Svarny, P., Tesar, M., Behrens, J. K., & Hoffmann, M. (2019, November). Safe physical HRI: Toward a unified treatment of speed and separation monitoring together with power and force limiting. In *2019 IEEE/RSJ International Conference on Intelligent Robots and Systems (IROS)* (pp. 7580-7587). IEEE.

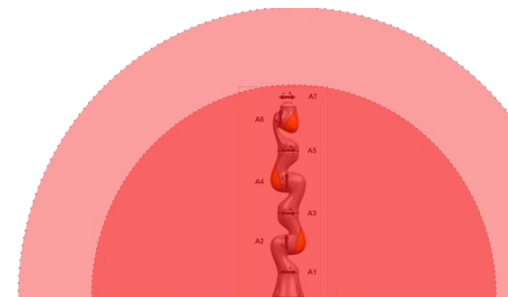
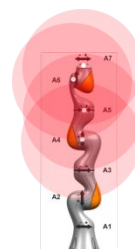
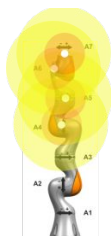
PFL & SSM



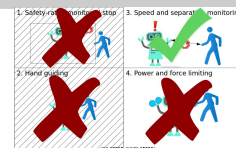
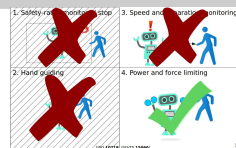
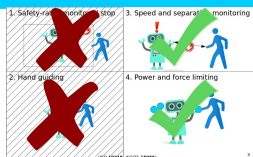
Svarny, P.; Tesar, M.; Behrens, J. K. & Hoffmann, M. (2019), Safe physical HRI: Toward a unified treatment of speed and separation monitoring together with power and force limiting, in 'Intelligent Robots and Systems (IROS), 2019 IEEE/RSJ International Conference on', IEEE, pp. 7574-7581.

SSM a PFL je nejrychlejší:

1. Vyšší takt neboť brzdí jen po PFL rychlost.
2. Pokračuje v práci i při zpomalení.

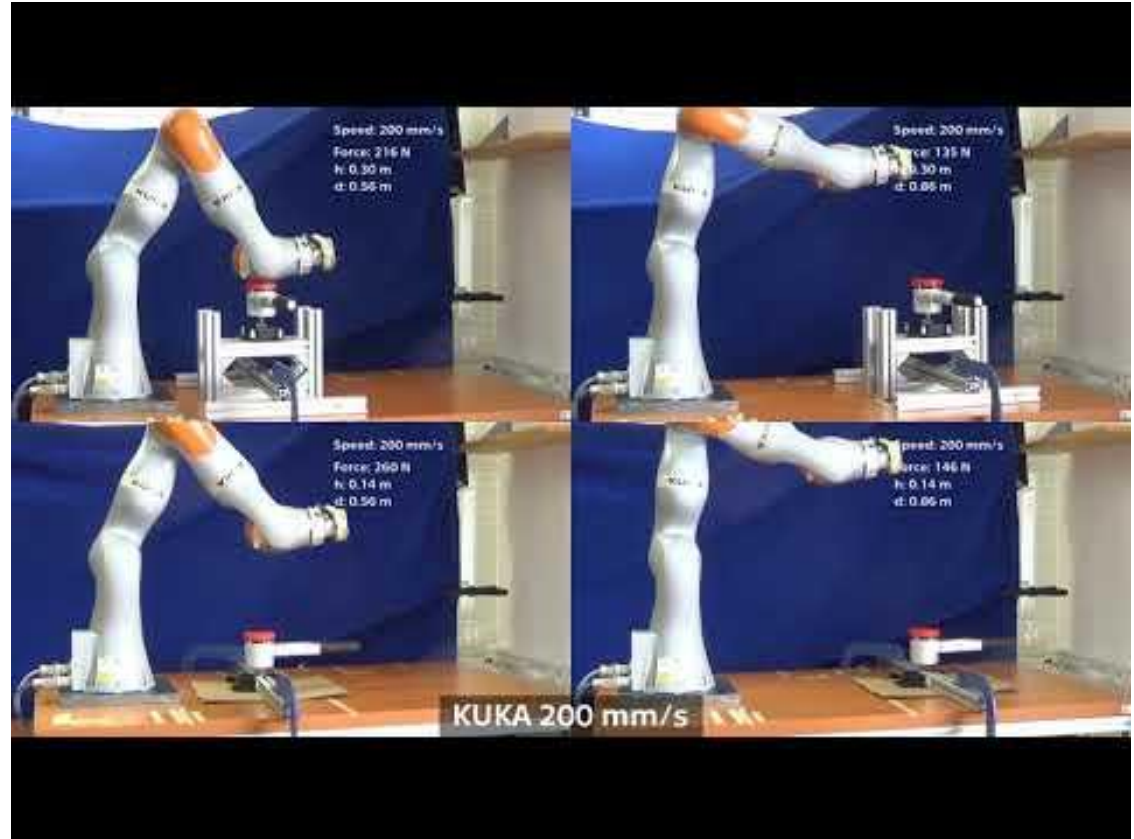


Naše	PFL	SSM	Stop
228 s	256 s	257 s	267 s



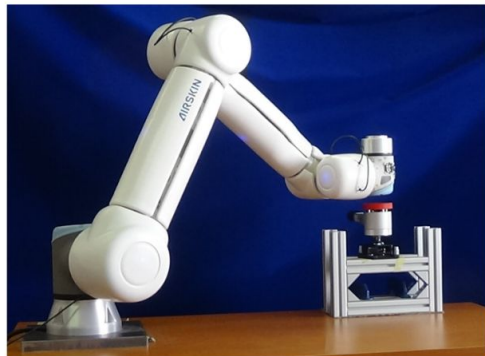
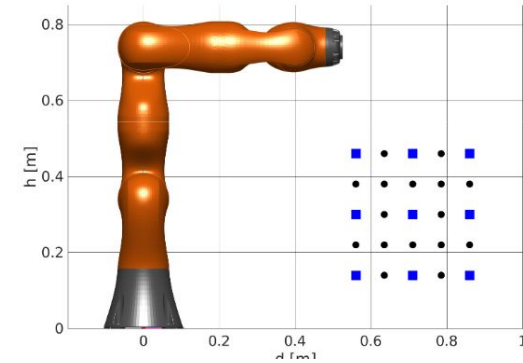
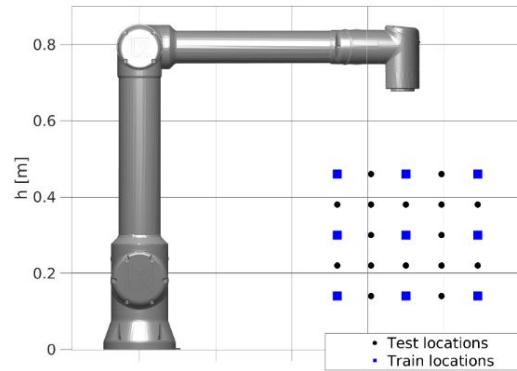
Reference (plná rychlost): 154 s

Případová studie - 3D Collision Force Map



Svarny, P., Rozlivek, J., Rustler, L., & Hoffmann, M. (2021, May). 3D Collision-Force-Map for Safe Human-Robot Collaboration. In *2021 IEEE International Conference on Robotics and Automation (ICRA)* (pp. 3829-3835). IEEE.

3D CFM - místa měření



(a) UR10e.



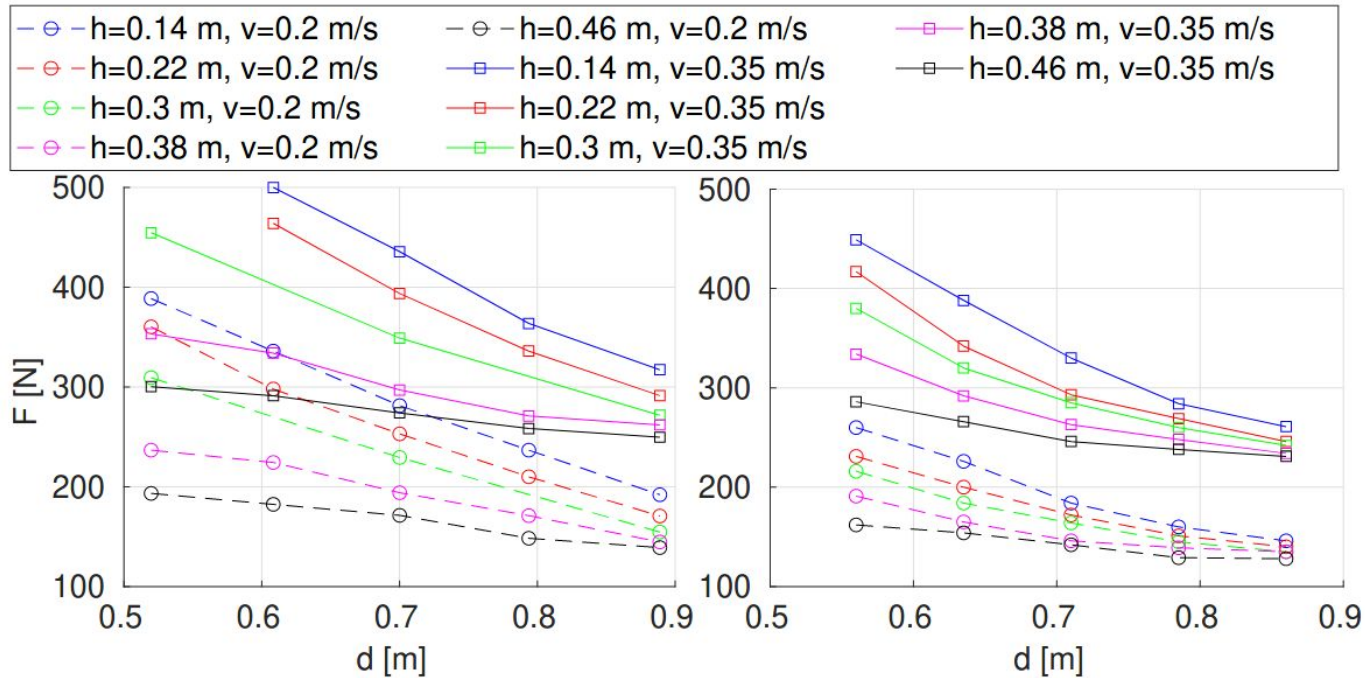
(b) KUKA LBR iiwa.

Fig. 1: Setup – robots and impact measuring device.

dataset	samples per state	training states (used samples*)	testing states (used samples*)
UR10e	3	27 (75)	88 (249)
KUKA 30 Nm	3	27 (78)	98 (291)
KUKA 10 Nm	1	27 (26)	98 (98)

Svarny, P., Rozlivek, J., Rustler, L., & Hoffmann, M. (2021, May). 3D Collision-Force-Map for Safe Human-Robot Collaboration. In *2021 IEEE International Conference on Robotics and Automation (ICRA)* (pp. 3829-3835). IEEE.

3D CFM - výsledky



UR10e

KUKA Ibr iiwa

3D CFM - předpověď nárazu

$$\ln(F) = \beta_0 + \beta_1 \cdot v + \beta_2 \cdot d + \beta_3 \cdot d^2 + \beta_4 \cdot d \cdot h + \beta_5 \cdot h^2 + \beta_6 \cdot d^2 \cdot v + \beta_7 \cdot d \cdot v^2 + \beta_8 \cdot d \cdot h^2$$

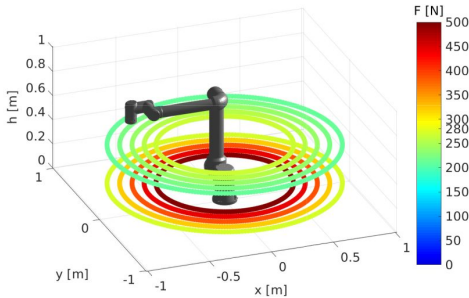
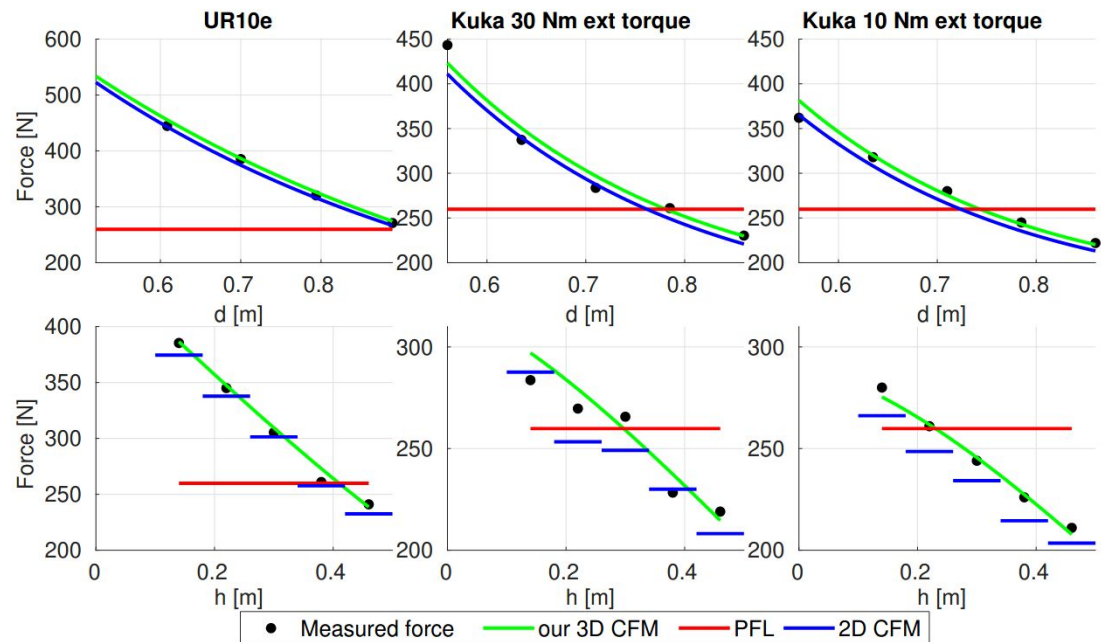


Fig. 6: UR10e – concentric impact force circles at various heights for end effector speed of 350 mm/s. Plotted are values from the 3D CFM model.

Svarny, P., Rozlivek, J., Rustler, L., & Hoffmann, M. (2021, May). 3D Collision-Force-Map for Safe Human-Robot Collaboration. In *2021 IEEE International Conference on Robotics and Automation (ICRA)* (pp. 3829-3835). IEEE.

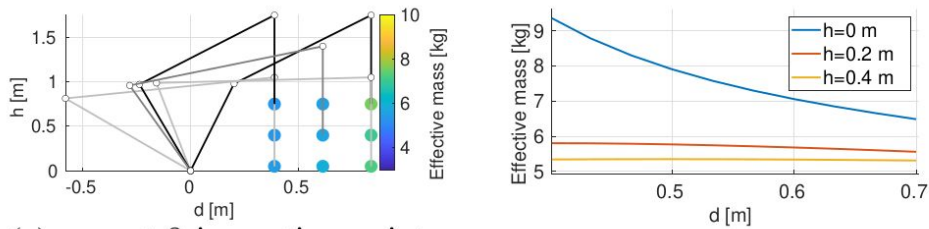
koncový efektor s rychlostí 0.30 m/s (směr dolů)



2D CFM - A. Schlotzhauer, L. Kaiser, J. Wachter, M. Brandstötter, and M. Hofbauer, "On the trustability of the safety measures of collaborative robots: 2D Collision-force-map of a sensitive manipulator for safe HRC," in 2019 IEEE 15th International Conference on Automation Science and Engineering (CASE). IEEE, 2019, pp. 1676–1683.

3D CFM - Problém s modelováním

Vliv konfigurace robota i materiálů na kolizi

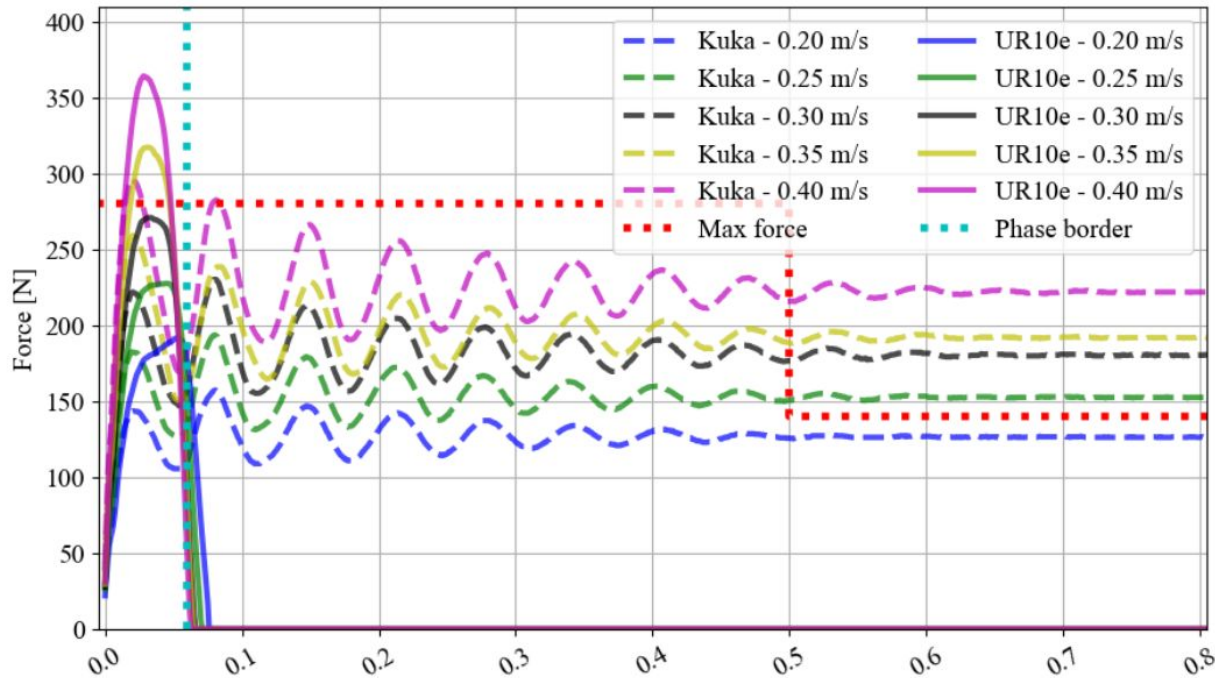


(a) m_R at 9 inspection points. (b) m_R as a function of d and h .

Fig. 4: Calculating effective mass of model 3 DoF planar manipulator. Collision direction “down”: $u = [0, -1]$.



3D CFM - potřeba měření v místě



Svarny, P., Rozlivek, J., Rustler, L., & Hoffmann, M. (2021, May). 3D Collision-Force-Map for Safe Human-Robot Collaboration. In *2021 IEEE International Conference on Robotics and Automation (ICRA)* (pp. 3829-3835). IEEE.

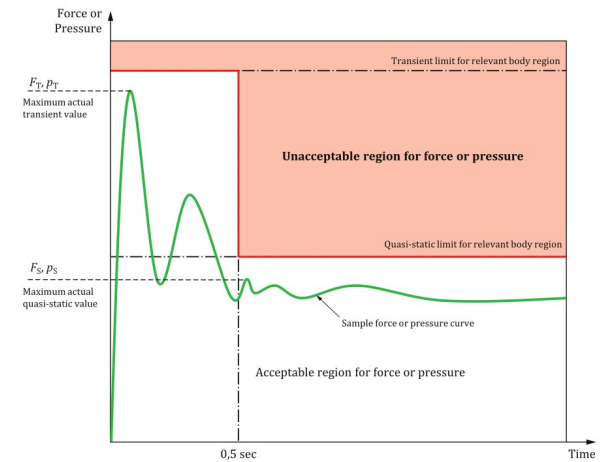


Figure 4 – Graphical representation of acceptable and unacceptable forces or pressures

ISO/TS 15066:2016
Robots and robotic devices – Collaborative robots

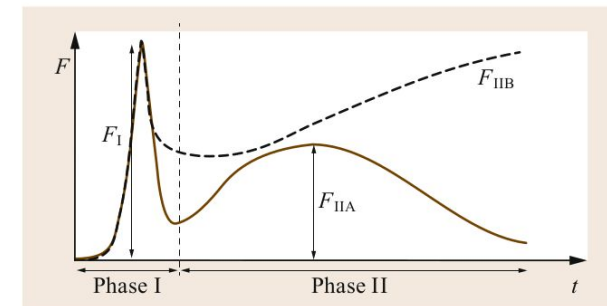
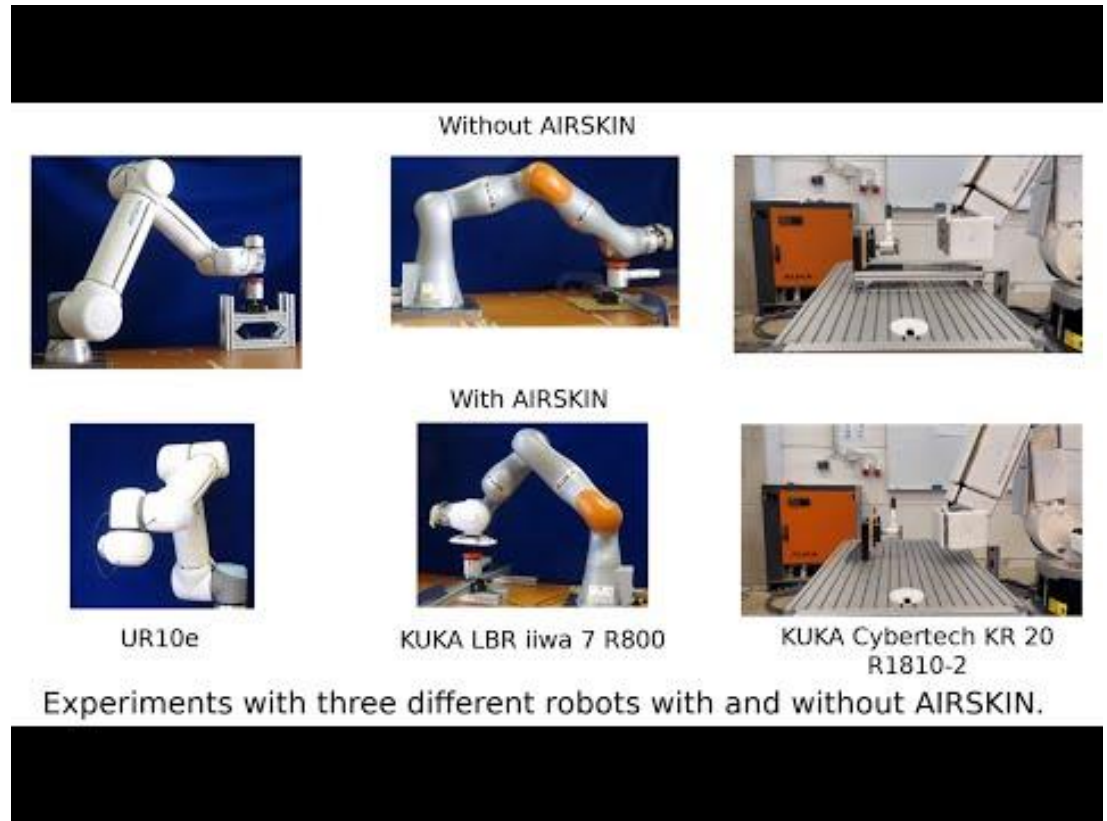


Fig. 69.6 Typical robot-human collision force profiles

Haddadin, S., & Croft, E. (2016). Physical human-robot interaction. In *Springer handbook of robotics* (pp. 1835-1874). Springer, Cham.

Případová studie Airskin - vliv materiálu



Svarny, P., Rozlivek, J., Rustler, L., Sramek, M., Deli, O., Zillich, M., & Hoffmann, M. (2022). Effect of Active and Passive Protective Soft Skins on Collision Forces in Human-robot Collaboration. *Robotics and Computer-Integrated Manufacturing*. [to appear]

Airskin - tuhost



(a) UR-skin



(b) The Pad

Figure 4: AIRSKIN pads with measurement grid.

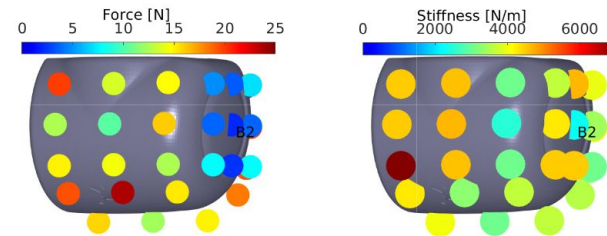


Figure 13: UR-skin threshold force (left) and stiffness (right). The measured values are color-coded. The impact point, B2, is also marked.

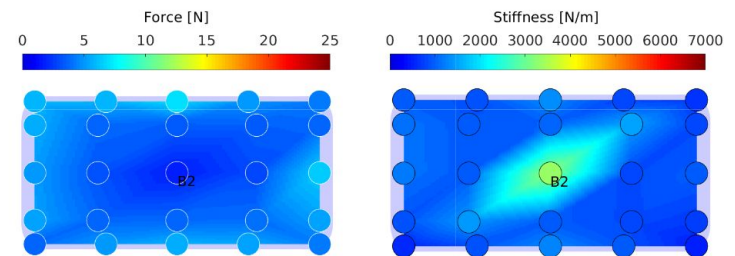


Figure 14: The Pad threshold force (left) and stiffness (right). The measured values are color-coded. The impact point, B2, is also marked.

Airskin - setup



(a) UR10e with AIRSKIN (transient contact).

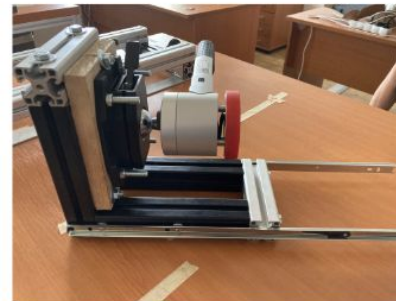


(b) KUKA iiwa with AIRSKIN module pad (quasi-static contact).

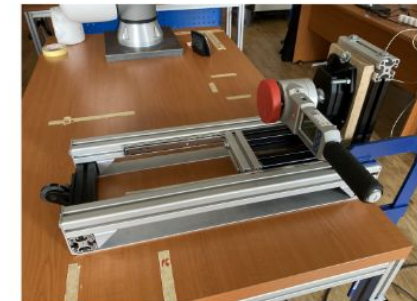


(c) KUKA Cybertech with AIRSKIN module pad (quasi-static contact).

Robot	Safety	Values		
UR10e	Preset	Pre-2	Pre-4	
	Skin	E-Stop	S-Stop	
KUKA iiwa	External torque	Stop 0	Stop 1	Stop 1 op
	Skin	Stop 0	Stop 1	Stop 1 op
KUKA Cybertech	Skin	Stop 1 op	Stop 2	



(a) Moving mass



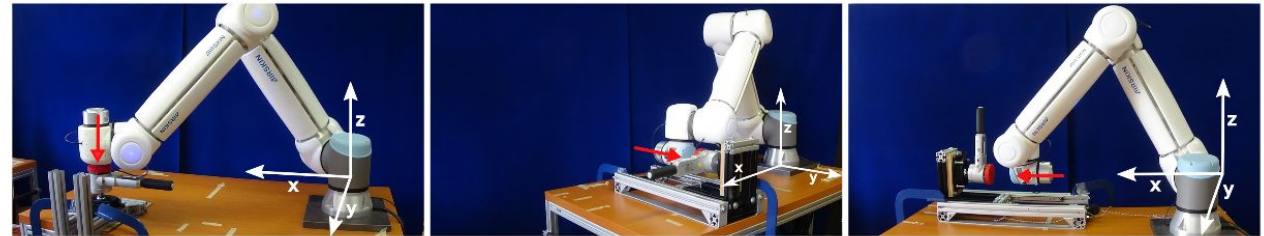
(b) Whole construction

Figure 3: Transient contact simulation construction.

Svarny, P., Rozlivek, J., Rustler, L., Sramek, M., Deli, O., Zillich, M., & Hoffmann, M. (2022). Effect of Active and Passive Protective Soft Skins on Collision Forces in Human-robot Collaboration. *Robotics and Computer-Integrated Manufacturing*, [to appear]

Airskin - pozice a směr

Place		Coordinates [m]			
Type	#	direction vector	UR10e	KUKA iiwa	KUKA Cybertech
quasi-static	0	$\begin{pmatrix} 0 \\ 0 \\ -1 \end{pmatrix}$	0.85 0.27 0.14	0.66 0.00 0.14	-
	1	$\begin{pmatrix} 0 \\ 1 \\ 0 \end{pmatrix}$	0.79 0.14 0.16	0.35 0.14 0.16	0.00 0.90 0.18
	2	$\begin{pmatrix} 1 \\ 0 \\ 0 \end{pmatrix}$	0.80 -0.22 0.16	0.37 -0.31 0.16	0.25 0.75 0.18
transient	3	$\begin{pmatrix} 0 \\ 1 \\ 0 \end{pmatrix}$	0.79 0.18 0.16	0.35 0.10 0.16	0.00 0.90 0.18
	4	$\begin{pmatrix} 1 \\ 0 \\ 0 \end{pmatrix}$	0.82 -0.22 0.16	0.33 -0.31 0.16	0.25 0.75 0.18



(a) Impact direction downward $(0, 0, -1)$, quasi-static case (b) Impact direction along the y -axis $(0, 1, 0)$, transient case (c) Impact direction along the x -axis $(1, 0, 0)$, transient case

Figure 5: Impact directions. The origin of the world reference frame is always at the base frame of the robot. The coordinates in the image are moved for visibility.

Table 3: World frame coordinates for the impact locations. The number # identifies the place, the direction vector is given in the world frame and the coordinates are given in the world frame. The origin of the world frame is located at the base frame of the robot.

Airskin - Stop kategorie dle ISO 13850

Stop 0 - okamžité zastavení, odpojení proudu a zapojení brzd.

Stop 1 - proud na zastavení, poté vypnut.

Stop 1 (path maintaining) - Stop Cat. 1 co musí zachovat i dráhu.

Stop 2 - zastavení pomocí ovladače, robot zůstává pod proudem. Bezpečnostní systém musí monitorovat a zajistit, že robot stojí.

Stop Category	UR10e	KUKA iiwa	KUKA Cybertech
Stop 0	Limit violation Fault detection	Stop 0	Stop 0
Stop 1	—	Stop 1	Stop 1
Stop 1 (path maintaining)	Emergency stop (E-stop)	Stop 1 op	Stop 1 op
Stop 2	Safeguard stop (S-stop)	—	Stop 2

Airskin - kolize podle zastavení a místa

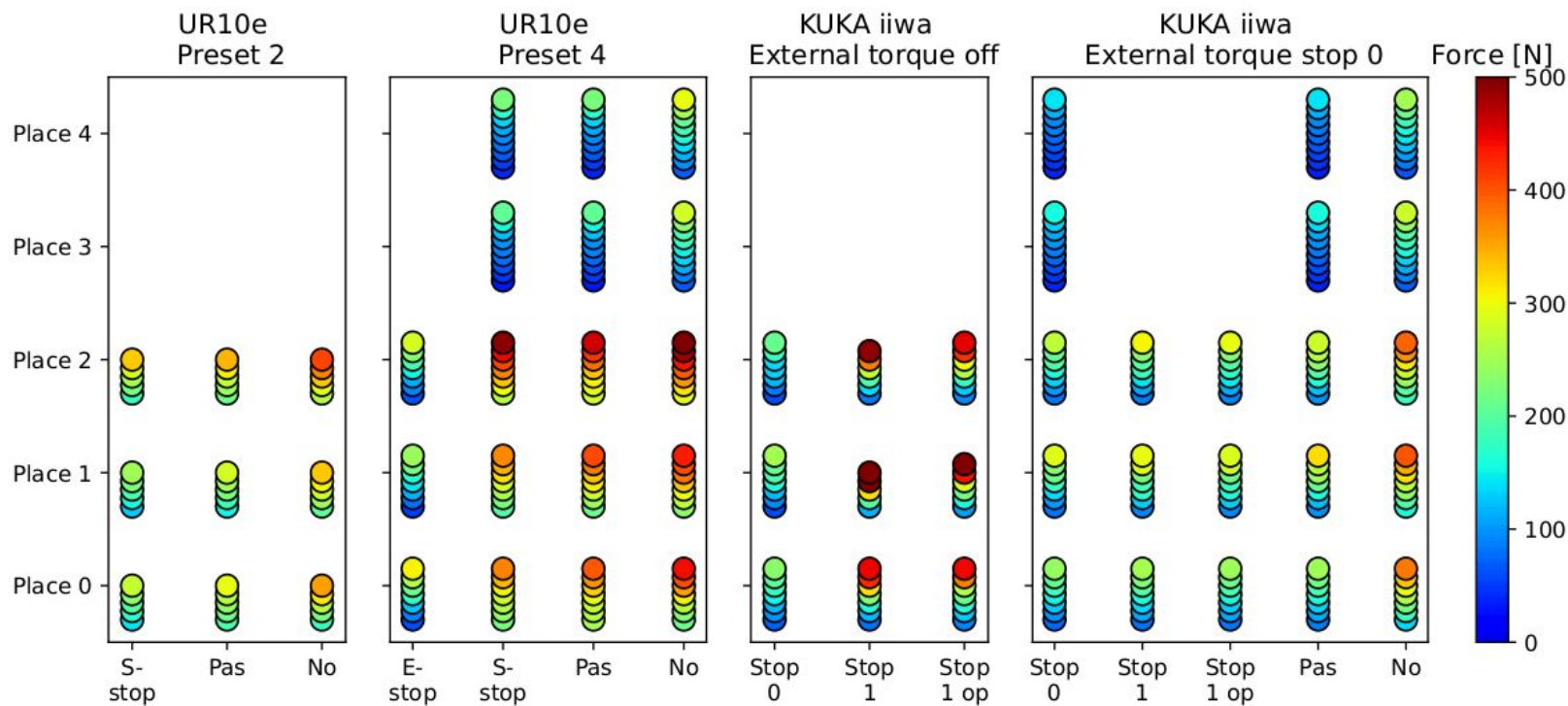


Figure 11: Peak impact forces comparison for the various UR10e and KUKA iiwa with various external torque settings. The circles represent the measured 7 velocities (from 0.2 to 0.5 m/s with increment 0.05 m/s), where applicable. The initiated stop behavior is either a Stop 0, Stop 1, or Stop 1 op on KUKA iiwa. For UR10e, these stops were Safeguard stop (S-stop) and Emergency stop (E-stop) and also the safety preset was considered (Pre-2 or Pre-4). The 'Pas' in the case of the AIRSKIN means the pads are pressurized but they do not initiate a stop, while 'No' means the AIRSKIN pad was removed from the robot. The three locations Place 0, 1, 2 are quasi-static collisions in the three directions downward, along y-axis, along x-axis respectively. The transient collisions along y-axis and along x-axis are Place 3, 4 respectively.

Airskin - KUKA iiwa - druhy zastavení

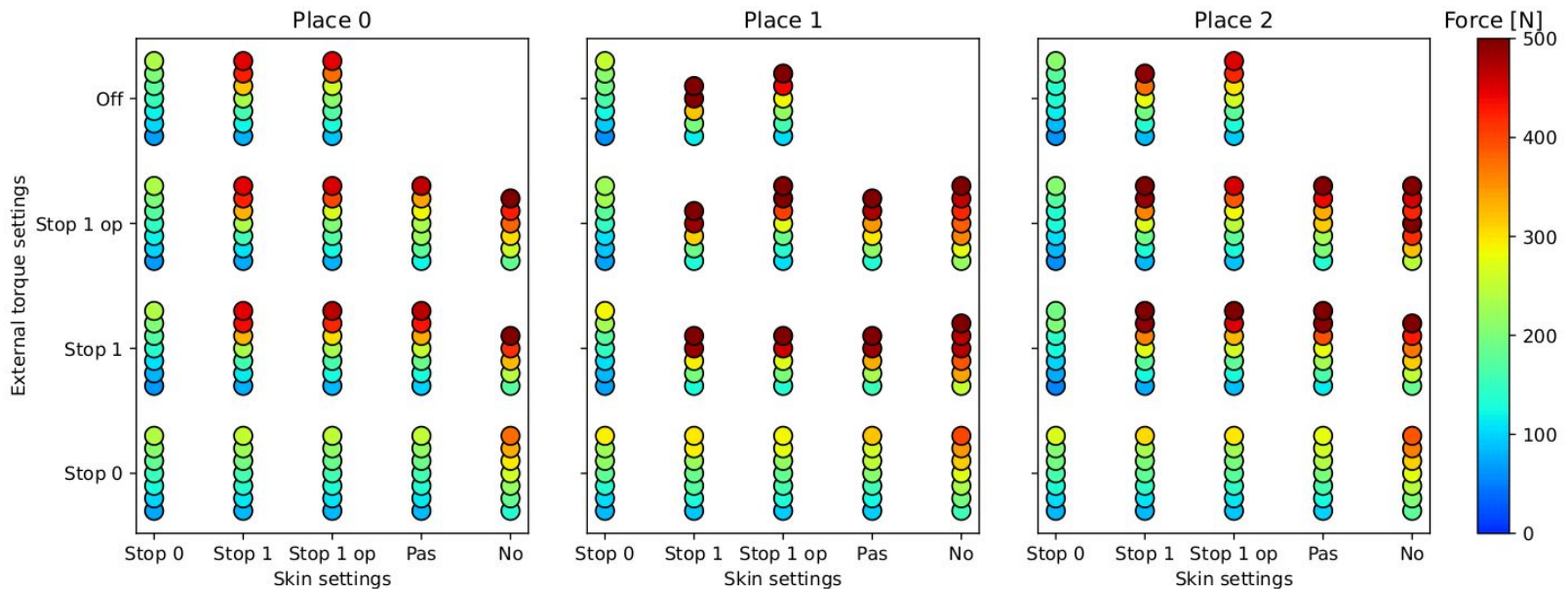


Figure 12: KUKA iiwa various stop combinations for quasi-static impacts. The initiated stop behavior is either a category 0 stop (Stop 0), a category 1 stop (Stop 1), a category 1 stop on path (Stop 1 op). The 'Pas' in the case of the AIRSKIN means the pads are pressurized but they do not initiate a stop, while 'No' means the AIRSKIN pad was removed from the robot. The 'Off' setting for the torques means that they were turned off. The circles represent the measured 7 velocities (from 0.2 to 0.5 m/s with increment 0.05 m/s), where applicable. The three locations Place 0, 1, 2 are downward, along y -axis, along x -axis respectively.

Airskin - silový profil

theory

ISO/TS 15066:2016
Robots and robotic
devices –
Collaborative robots

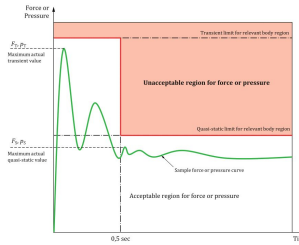


Figure 4 – Graphical representation of acceptable and unacceptable forces or pressures

Haddadin, S., & Croft, E. (2016). Physical human-robot interaction. In *Springer handbook of robotics* (pp. 1835-1874). Springer, Cham.

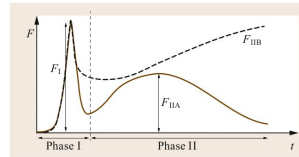
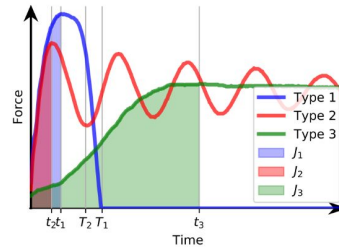
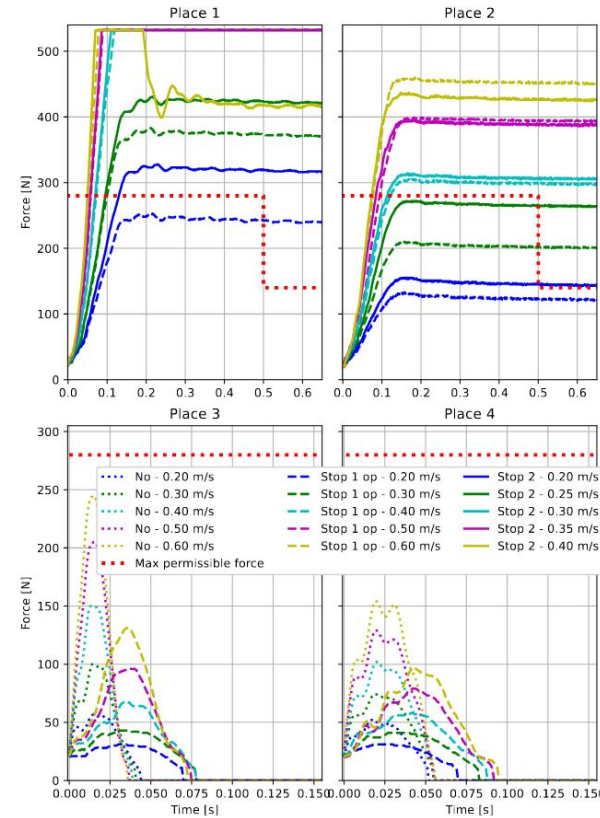


Fig. 69.6 Typical robot-human collision force profiles



quasi-static



KUKA Cybertech

quasi-static contact,
0.3 m/s, place 2
KUKA iiwa, UR10e

transient

Svarny, P., Rozlivek, J., Rustler, L., Sramek, M., Deli, O., Zillich, M., & Hoffmann, M. (2022). Effect of Active and Passive Protective Soft Skins on Collision Forces in Human-robot Collaboration. *Robotics and Computer-Integrated Manufacturing*. [to appear]

Airskin - výsledky

Svarny, P., Rozlivek, J., Rustler, L., Sramek, M., Deli, O., Zillich, M., & Hoffmann, M. (2022). Effect of Active and Passive Protective Soft Skins on Collision Forces in Human-robot Collaboration.

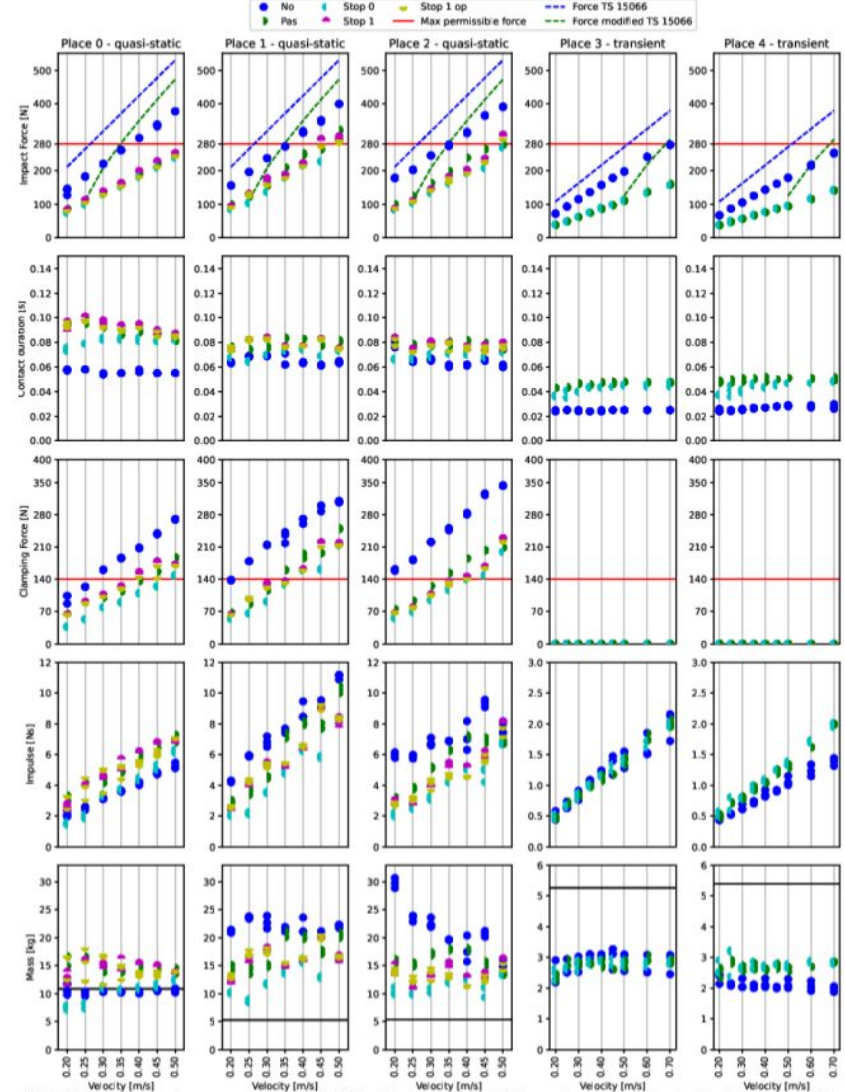
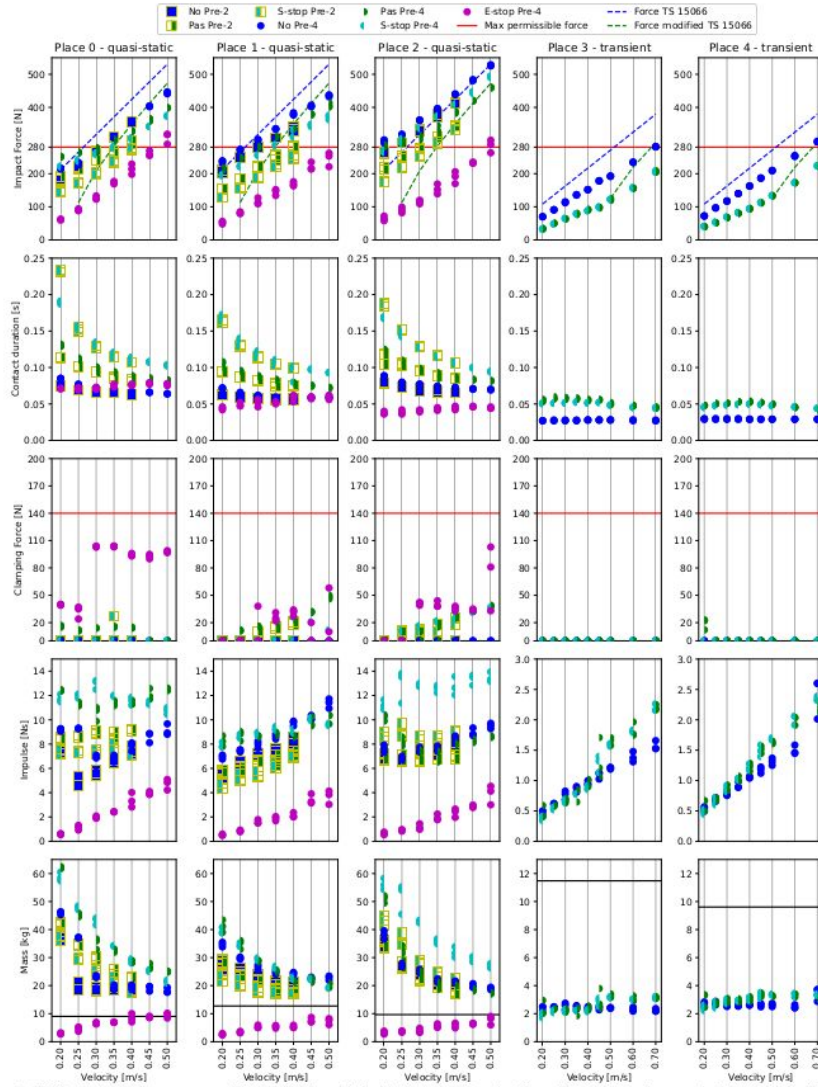


Figure 7: UR10e summary of measurements. The AIRSKIN module is either absent (No), active (S-stop/E-stop) or merely pressurized but not active (Pas). The robot is either in the least restrictive preset (Pre-4) or in the second most restrictive preset (Pre-2). In addition, active skin could trigger either the safeguard stop (S-stop) or the emergency stop (E-stop). The duration is the time between the impact detection and the first local minimum of the force measurement, i.e., the end of Phase I. The maximum permissible force is derived from TS 15066. Dashed lines are force predictions from Eq. (7) – see Sec. 2.4. The effective mass is calculated from the UR10e model.

Figure 9: KUKA iiwa summary of measurements. The AIRSKIN module is either absent (No), merely pressurized but not active (Pas) or active with various stopping behaviors (Stop 0, Stop 1, Stop 1 op). The maximum permissible force is derived from TS 15066. Dashed lines are force predictions from Eq. (7) – see Sec. 2.4. The duration is the time between the impact detection and the first local minimum of the force measurement, i.e., the end of Phase I. The effective mass is calculated from the KUKA iiwa model.

Airskin - model padu

ISO/TS 15066

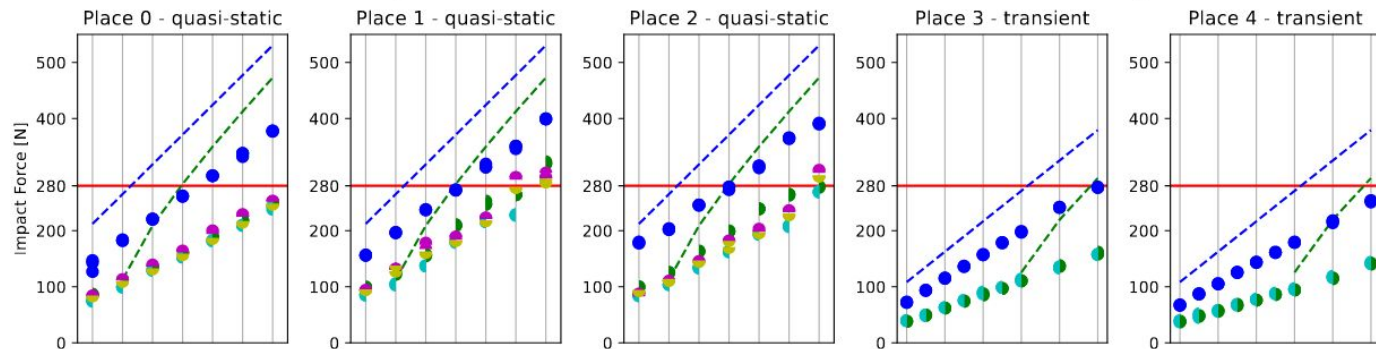
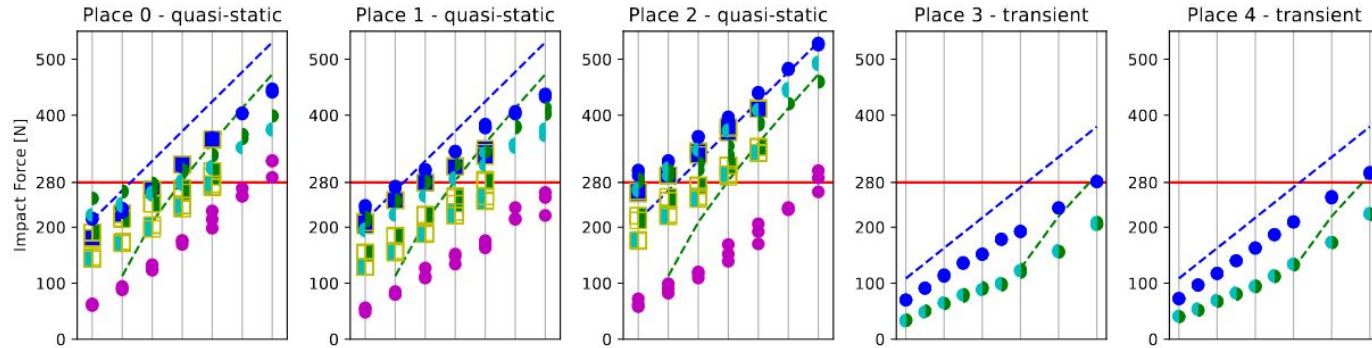
$$v \leq \frac{F_{\max}}{\sqrt{k}} \sqrt{m_R^{-1} + m_H^{-1}} = \frac{F_{\max}}{\sqrt{k \cdot \mu}},$$

Soft cover model

$$v \leq \sqrt{\frac{F_{\max}^2}{k \cdot \mu} + \frac{d_s^2 \cdot k_s}{\mu}}$$

Svarny, P., Rozlivek, J., Rustler, L., Sramek, M., Deli, O., Zillich, M., & Hoffmann, M. (2022). Effect of Active and Passive Protective Soft Skins on Collision Forces in Human-robot Collaboration. *Robotics and Computer-Integrated Manufacturing*. [to appear]

Airskin - model padu



Koboti

- dobrý nápad, co ještě hledá své místo.

Bezpečnost

- vždy se ověřuje aplikace v místě.

Děkuji za pozornost

